

# The Increased Trafficking of the Calcium Channel Subunit $\alpha_2\delta$ -1 to Presynaptic Terminals in Neuropathic Pain Is Inhibited by the $\alpha_2\delta$ Ligand Pregabalin

Claudia S. Bauer,<sup>1</sup> Manuela Nieto-Rostro,<sup>1</sup> Wahida Rahman,<sup>1</sup> Alexandra Tran-Van-Minh,<sup>1</sup> Laurent Ferron,<sup>1</sup> Leon Douglas,<sup>1</sup> Ivan Kadurin,<sup>1</sup> Yorain Sri Ranjan,<sup>1</sup> Laura Fernandez-Alacid,<sup>2</sup> Neil S. Millar,<sup>1</sup> Anthony H. Dickenson,<sup>1</sup> Rafael Lujan,<sup>2</sup> and Annette C. Dolphin<sup>1</sup>

<sup>1</sup>Department of Neuroscience, Physiology and Pharmacology, University College London, London WC1E 6BT, United Kingdom, and <sup>2</sup>Departamento Ciencias Medicas, Universidad de Castilla-La Mancha, 02006 Albacete, Spain

Neuropathic pain results from damage to the peripheral sensory nervous system, which may have a number of causes. The calcium channel subunit  $\alpha_2\delta$ -1 is upregulated in dorsal root ganglion (DRG) neurons in several animal models of neuropathic pain, and this is causally related to the onset of allodynia, in which a non-noxious stimulus becomes painful. The therapeutic drugs gabapentin and pregabalin (PGB), which are both  $\alpha_2\delta$  ligands, have antiallodynic effects, but their mechanism of action has remained elusive. To investigate this, we used an *in vivo* rat model of neuropathy, unilateral lumbar spinal nerve ligation (SNL), to characterize the distribution of  $\alpha_2\delta$ -1 in DRG neurons, both at the light- and electron-microscopic level. We found that, on the side of the ligation,  $\alpha_2\delta$ -1 was increased in the endoplasmic reticulum of DRG somata, in intracellular vesicular structures within their axons, and in the plasma membrane of their presynaptic terminals in superficial layers of the dorsal horn. Chronic PGB treatment of SNL animals, at a dose that alleviated allodynia, markedly reduced the elevation of  $\alpha_2\delta$ -1 in the spinal cord and ascending axon tracts. In contrast, it had no effect on the upregulation of  $\alpha_2\delta$ -1 mRNA and protein in DRGs. *In vitro*, PGB reduced plasma membrane expression of  $\alpha_2\delta$ -1 without affecting endocytosis. We conclude that the antiallodynic effect of PGB *in vivo* is associated with impaired anterograde trafficking of  $\alpha_2\delta$ -1, resulting in its decrease in presynaptic terminals, which would reduce neurotransmitter release and spinal sensitization, an important factor in the maintenance of neuropathic pain.

## Introduction

Neuropathic pain results from nerve damage, which may have several different origins, including trauma, diabetes, herpes infection, and cancer. Its phenotype involves hyperalgesia, allodynia, and spontaneous pain (Dickenson et al., 2002). There are several well established animal models of neuropathic pain including unilateral spinal nerve ligation (SNL) (Kim and Chung, 1992; Bennett et al., 2003), in which a plethora of genes change their expression in the damaged dorsal root ganglion (DRG) neurons (Costigan et al., 2002; Wang et al., 2002). These changes include a significant upregulation of the calcium channel accessory subunit  $\alpha_2\delta$ -1 (for review, see Davies et al., 2007). Increased expression has been observed for  $\alpha_2\delta$ -1 mRNA in DRGs (Newton et al., 2001; Wang et al., 2002) and for  $\alpha_2\delta$ -1 protein, in both the

affected ganglia and the spinal cord dorsal horn (Li et al., 2004). This increase of  $\alpha_2\delta$ -1 coincides with the onset of tactile allodynia (Li et al., 2004).

Evidence that elevation of the  $\alpha_2\delta$ -1 subunit has significant relevance to the development of neuropathic pain is first that mice globally overexpressing  $\alpha_2\delta$ -1 exhibit tactile allodynia in the absence of nerve damage (Li et al., 2006). Second, the antiallodynic and antihyperalgesic gabapentinoid drugs pregabalin (PGB) and gabapentin are of important therapeutic benefit in the treatment of neuropathic pain and have been shown to be  $\alpha_2\delta$  ligands (Brown et al., 1998; Field et al., 2006). Third, knock-in mice expressing a mutant  $\alpha_2\delta$ -1 subunit that does not bind gabapentinoids develop neuropathic pain that is insensitive to these drugs (Field et al., 2006). Nevertheless, to date, no molecular mechanism has been put forward to account for the ability of these drugs to alleviate neuropathic pain *in vivo*.

Voltage-gated calcium channels of the  $Ca_v1$  and  $Ca_v2$  classes can be purified as heteromeric complexes consisting of an  $\alpha_1$  subunit, associated with a  $\beta$  and an  $\alpha_2\delta$  subunit (for review, see Catterall, 2000; Dolphin, 2003). The principal effect of calcium channel  $\alpha_2\delta$  subunits is to increase the functional expression of these channels (Jones et al., 1998; Qin et al., 1998; Wyatt et al., 1998; Barclay et al., 2001; Klugbauer et al., 2003), as a consequence of increased trafficking (Cantí et al., 2005). Recently, we showed that gabapentin only produces a substantial inhibition of

Received Jan. 22, 2009; accepted Feb. 19, 2009.

This work was supported by Biotechnology and Biological Sciences Research Council Grant BB D018250 (supporting C.S.B. and W.R.) (A.H.D., A.C.D., N.S.M.); Medical Research Council Grant G0700368 (supporting L.D.) (A.C.D.), Wellcome Trust Grant GR077883MA (supporting M.N.-R. and L.F.) (A.C.D.), and Epilepsy Research UK (supporting I.K.) (A.C.D.); and Junta de Comunidades de Castilla la Mancha Grant PAI08-0174-6967 (R.L.). A.T.-V.-M. holds a University College London PhD Scholarship. We thank K. Chaggar, L. Bee, and J.-L. Vonsy for technical assistance.

Correspondence should be addressed to either Claudia S. Bauer or Annette C. Dolphin, Laboratory of Cellular and Molecular Neuroscience, Department of Neuroscience, Physiology and Pharmacology, Andrew Huxley Building, University College London, Gower Street, London WC1E 6BT, UK. E-mail: c.bauer@ucl.ac.uk or a.dolphin@ucl.ac.uk.

DOI:10.1523/JNEUROSCI.0356-09.2009

Copyright © 2009 Society for Neuroscience 0270-6474/09/294076-13\$15.00/0

calcium currents when applied chronically but not acutely *in vitro*, by reducing the expression of  $\text{Ca}_v\alpha 1$  and  $\alpha_2\delta$  subunits at the plasma membrane (PM) (Hendrich et al., 2008). We concluded that gabapentin is an inhibitor of calcium channel trafficking.

In the present study, we used a rat model of neuropathic pain (lumbar L5/L6 SNL) to test our hypothesis that gabapentinoid drugs inhibit the trafficking of  $\alpha_2\delta$ -1 from DRG cell bodies to their presynaptic terminals in the dorsal horn of the spinal cord. We analyzed the distribution of  $\alpha_2\delta$ -1 in DRGs, axons, and spinal cord in the ligated L5/L6 region compared with the nonligated L4 region, both at the light- and electron-microscopic (EM) level, and we determined the effect of chronic PGB treatment on  $\alpha_2\delta$ -1 distribution. We found that chronic PGB treatment at a dose that alleviated neuropathic pain also inhibited the anterograde trafficking of  $\alpha_2\delta$ -1 subunits.

## Materials and Methods

**Nerve injury-selective (L5/6) spinal nerve ligation.** A total of 48 male Sprague Dawley rats (Central Biological Services, University College London, London, UK) weighing 130–150 g at time of surgery was used for this study. All experimental procedures were approved by the United Kingdom Home Office and followed the guidelines of the International Association for the Study of Pain (Zimmermann, 1983). Selective SNL surgery was conducted as previously described (Kim and Chung, 1992). Briefly, the left L5 and L6 spinal nerves were isolated and tightly ligated with 6-0 silk thread under isoflurane anesthesia (50%  $\text{O}_2$ /50%  $\text{N}_2\text{O}$ ). Hemostasis was confirmed and the wound was sutured. Sham operations were performed in the same way except that spinal nerves were not ligated. After surgery, the animals were allowed to recover and housed at a maximum of five per cage. Food and water were available *ad libitum*. The foot posture and general behavior of the operated rats were monitored throughout the postoperative period. Animals with impaired motor activity were omitted from this study.

**Drug administration.** PGB (a gift from Pfizer) was dissolved in 0.9% saline solution to give a dose of 30 mg/kg. After recovery from surgery, rats were divided into two groups and randomly assigned to receive either PGB or saline injections (SNL plus PGB or SNL plus saline, respectively). All injections were administered subcutaneously in the scruff of the back of the neck. Beginning on postoperative day 1, rats were given three daily injections of either PGB or saline until postoperative day 9 when the animals were culled 1 h after the second injection. Animals used to investigate the accumulation of  $\alpha_2\delta$ -1 at the ligation side were killed on postoperative day 4.

**Behavioral observations.** Behavioral responses to mechanical and cooling stimulation of the ipsilateral and contralateral hindpaws were recorded preoperatively and postoperatively on days –3, 2, 4, 7, and 9 and conducted 1 h after a PGB injection. Briefly, animals were left to acclimatize to the area for 30 min before testing. Sensitivity to mechanical punctate stimulation (response frequency) was assessed through the measurement of the number of foot withdrawal responses to a trial of 10 applications of calibrated hand-held von Frey filaments with increasing bending force of 2, 6, and 8 g corresponding to ~19.6, 58.9, and 78.5 mN (Touch-Test; North Coast Medical) to the plantar surface of each hindpaw. Sensitivity to cooling stimulation was similarly assessed as the number of withdrawals of a trial of five applications of a drop of acetone to the plantar surface of ipsilateral and contralateral hindpaws. Response frequency was quantified as the number of foot withdrawals per 10 or 5 trials, respectively. The dose of PGB used in the present study (30 mg/kg, s.c.) has been reported not to produce any sedative effects (Field et al., 2001). To assess possible sedative effects of the multiple dosing regimen, performance on a rotarod (Ugo Basile model 7750; Linton Instruments) was also recorded. The apparatus was set to accelerate from 0 to 20 rpm over 60 s and the time maintained on the beam before falling was recorded (with a maximum cutoff of 150 s). Only rats scoring between 60 and 120 s in the two training sessions before surgery were used for exper-

imentation. Spinal nerve ligation itself had no adverse effect on the rotarod performance when compared with sham-operated rats [time on the rotarod 3 d before surgery: SNL,  $93 \pm 9$  s ( $n = 14$ ); sham,  $90 \pm 8$  s ( $n = 11$ ); time on the rotarod 7 d after surgery: SNL,  $62 \pm 14$  s ( $n = 14$ ); sham,  $76 \pm 10$  s ( $n = 11$ )]. The statistical significance of differences between data was determined using the nonparametric Mann–Whitney *U* test (GraphPad Prism 4.0). The level of significance was set to  $*p < 0.05$ .

**Quantitative PCR and immunoblotting.** For quantitative PCR (Q-PCR) and immunoblot assays, the methods used were essentially as described previously (Davies et al., 2006; Donato et al., 2006). Briefly, RNA was extracted from individual ipsilateral or contralateral L4 or pooled L5 and L6 pulverized frozen DRGs, 7–14 d after ligation or 14 d after sham surgery and from ipsilateral or contralateral DRGs obtained from SNL plus PGB- or SNL plus saline-injected animals. RNA was also extracted from ipsilateral and contralateral spinal cord dorsal horn tissue 4 d after SNL. RNA was isolated using RNeasy columns (QIAGEN), including an on-column DNase step. Reverse transcription was performed on 1  $\mu\text{g}$  of RNA using the iScript kit with random primers (Bio-Rad). Q-PCR was performed with an iCycler (Bio-Rad) using the iQ SYBR supermix (Bio-Rad). For each set of primers and for every experiment, a standard curve was generated using a serial dilution of reverse-transcribed RNA from the combined samples. Data were normalized for expression of glyceraldehyde-3-phosphate dehydrogenase (GAPDH) mRNA. Data from the ipsilateral side were then normalized to their respective contralateral side, if not stated otherwise, and given as the mean  $\pm$  SEM. Statistical significance between sham, 7 or 14 d SNL and SNL plus saline and SNL plus PGB conditions of ipsi (5 + 6) or ipsi 4 DRGs was determined by a one-way ANOVA test with Student–Newman–Keuls (SNK) post test (GraphPad Prism). Data from Q-PCR on spinal cord tissue were normalized to the  $\alpha_2\delta$ -1 mRNA level in contralateral L5 DRGs measured in parallel, and statistical significance was determined by Student's nonpaired *t* test. The following Q-PCR primers were used: rat GAPDH (AF\_106860), 5'-ATGACTCTACCCACGGCAAG-3', 5'-CATACTCTGCACCAGCATCTC-3'; rat  $\alpha_2\delta$ -1 (NM\_012919), 5'-AGCCTATGTGCCATCAATTAC-3', 5'-AGTCATCCTCTTCCATTCAAC-3'; rat  $\alpha_2\delta$ -2 (NM\_175592), 5'-CAGTGGTGGGTGTCAAAC-3', 5'-TACCTCGCAGTCCATCTC-3'; rat  $\alpha_2\delta$ -3 (NM\_175595), 5'-TCCGAACGCACCATCAAG-3' (forward), 5'-ACTGTCCACCACCACCAT-3' (reverse).

For immunoblotting, proteins were extracted from 1 mm spinal nerve segments, complete DRGs, and 8–10 mm dorsal root segments pooled from two to four animals in a buffer of PBS with 1 mM EDTA in the presence of protease inhibitors (Complete; Roche Diagnostics) by sonication (2–3 s) followed by incubation with 0.2% SDS and 1% Igepal for 40 min on ice. After centrifugation (30 min at  $14,000 \times g$  at 4°C), 14  $\mu\text{g}$  of protein per sample were loaded onto a 3–8% NuPage Tris/acetate gel (Invitrogen), and proteins were separated by SDS-PAGE. Proteins were transferred to poly(vinylidene difluoride) membranes (Bio-Rad) and, after blocking (500 mM NaCl, 10 mM Tris, pH 7.4, with 3% BSA and 0.5% Igepal), were probed with the mouse monoclonal anti-dihydropyridine receptor ( $\alpha_2$ -1 subunit) antibody (1:1000; Sigma-Aldrich) at room temperature (RT) overnight or with the mouse monoclonal anti-GAPDH antibody (1:37,500; Ambion) for 1 h. The protein–antibody complexes were then labeled with a horseradish peroxidase-conjugated secondary antibody (1:2000; Sigma-Aldrich) for 1 h at RT and detected using the enhanced ECL Plus reagent (GE Healthcare) visualized with a Typhoon 9410 scanner (GE Healthcare). Quantification of immunoblot bands was performed with ImageQuant software (GE Healthcare).

**Immunocytochemistry.** To validate the specificity of the mouse monoclonal anti-dihydropyridine receptor ( $\alpha_2$ -1 subunit) antibody (Sigma-Aldrich), Cos-7 cells were transfected with either rat  $\alpha_2\delta$ -1 (AF\_286488) or mouse  $\alpha_2\delta$ -2 (AF\_247139) in conjunction with rat  $\beta 1b$  (X61394) and rabbit  $\text{Ca}_v2.2$  (D14157) as described previously (Page et al., 2004). The immunocytochemical detection of  $\alpha_2\delta$ -1 was performed as described previously (Cantí et al., 2005). Briefly, extracellular immunoreactivity was detected by incubating nonpermeabilized cells with mouse anti- $\alpha_2\delta$ -1 antibody (1:100) in growth medium for 1 h at 37°C. Cells were fixed with 4% paraformaldehyde in PBS for 5 min at RT. For labeling of intracellular epitopes, cells were permeabilized for 15 min with 0.02% Triton X-100 in Tris-buffered saline (TBS); for nonpermeabilized cells,

this step was omitted. All cells were then blocked for at least 30 min in TBS with 20% goat serum (GS) and 4% BSA and incubated with the anti- $\alpha_2\delta$ -1 antibody (1:100) at 4°C overnight. Samples were then washed and incubated with biotinylated goat anti-mouse IgG (1:500; Invitrogen) for 2 h at RT followed by streptavidin-Alexa Fluor 488 (1:500; Invitrogen) for 1 h at RT. After washing and DNA staining with 4',6-diamidino-2-phenylindole (DAPI) (300 nM; Invitrogen), samples were mounted in VectaShield (Vector Laboratories). To test for cross-reactivity, permeabilized cells expressing  $\alpha_2\delta$ -2 were incubated with a mixture of the mouse monoclonal anti- $\alpha_2\delta$ -1 antibody (1:100) and a rabbit polyclonal anti- $\alpha_2\delta$ -2 antibody [ $\alpha_2$ -2 (107–117); 0.55  $\mu$ g/ml] (Brodbeck et al., 2002) at 4°C overnight. The primary antibodies were recognized with biotinylated goat anti-mouse IgG and streptavidin-Alexa Fluor 488 or with anti-rabbit-Texas Red antibody (Invitrogen). Immunofluorescence labeling was detected with a LSM 510Meta (Zeiss) confocal microscope. Experiments were performed on at least two individual transfections.

To investigate the effect of PGB on cell surface expression of  $\alpha_2\delta$ -1, 20 or 200  $\mu$ M PGB dissolved in 0.9% saline was added to the growth medium at the time of transfection. An equal volume of saline was added to control cells. The extracellular immunoreactivity was then detected in nonpermeabilized cells as described above.

Endocytosis of  $\alpha_2\delta$ -1 in Cos-7 cells coexpressing  $\alpha_2\delta$ -1,  $Ca_v2.2$ , and  $\beta 1b$ , 72 h after transfection and incubation in absence or presence of 200  $\mu$ M PGB was measured by labeling cells with the mouse monoclonal anti- $\alpha_2$ -1 antibody (1:150) at 37°C for 2.5 h (with PGB present when required). Cells were then fixed, and cell surface  $\alpha_2\delta$ -1 subunits were detected in the absence of permeabilization with a Texas Red-conjugated secondary antibody (1:100) mixed with a nonlabeled secondary antibody (1:500) for saturation. The cells were then permeabilized with 0.02% Triton X-100 and internalized antibody was detected with an Alexa Fluor 488-conjugated secondary antibody (1:500). Images were acquired as described above. Experiments were performed on three individual transfections.

**Immunohistochemistry.** Rats were deeply anesthetized with an intraperitoneal injection of (600 mg/kg) pentobarbitone (Euthatal; Merial Animal Health), perfused transcardially with saline containing heparin followed by perfusion with 4% paraformaldehyde in 0.1 M phosphate buffer (PB), pH 7.4. Ipsilateral and contralateral L4–6 DRGs with the adjacent spinal nerve and dorsal root, L4–6 lumbar and upper cervical spinal cord, and the brainstem were dissected out. The tissue was post-fixed for 1.5–2 h, washed with PB, cryoprotected by incubation in PB with 15% sucrose overnight, and finally frozen before sectioning with a cryostat. DRGs were sectioned to a thickness of 10  $\mu$ m and spinal cord to 15  $\mu$ m. For immunofluorescence labeling, a modification of a method described previously was used (Li et al., 2006). Sections underwent heat-induced antigen retrieval (10 mM citrate buffer, pH 6.0, 0.05% Tween 20, 95°C for 10 min) before blocking with 10% GS in the presence of 0.1% Triton X-100 in PBS for 1 h. To detect  $\alpha_2\delta$ -1, sections were incubated with the mouse monoclonal anti- $\alpha_2$ -1 antibody (1:100) in 50% blocking buffer for 40 h at 4°C. After extensive washing with PBS containing 0.1% Triton X-100, sections were incubated with biotinylated goat anti-mouse IgG (1:500) for 2 h at RT and streptavidin-Alexa Fluor 488 (1:500) for 1 h at RT. After extensive washing and DNA staining with DAPI, samples were mounted in VectaShield (Vector Laboratories). For immunoperoxidase staining, endogenous peroxidase was blocked with 3%  $H_2O_2$  for 30 min before antigen retrieval. Sections were blocked using the Vectastain Elite ABC kit (Vector Laboratories), incubated with the primary and secondary antibody (ABC kit) for 2 h followed by 1 h incubation with the avidin–biotin complex (ABC kit). Peroxidase activity was detected with diaminobenzidine according to the manufacturer's protocol (Vector Laboratories). After extensive washing, samples were dehydrated, cleared, and mounted in DPX (distyrene, plasticizer, and xylene) (Sigma-Aldrich). All experiments were performed on frozen sections with the exception of paraffin-embedded sections shown in Figure 2. For paraffin embedding, tissue was dehydrated in ethanol, treated with Histoclear (Thermo Fisher Scientific), and infiltrated with paraffin (VWR) at 65°C overnight. Paraffin blocks were sectioned on a microtome at 10  $\mu$ m thickness. Sections were then deparaffinized and rehydrated, and underwent immunoperoxidase staining as described above. The anatomical

position of the brainstem sections is based on the rat atlas of Paxinos and Watson (2005). The immunohistochemical staining of  $\alpha_2\delta$ -1 in dorsal roots (see Fig. 5) was performed on intact tissue. Dorsal roots were removed 2–7 d after ligation and fixed in 4% PFA in 0.1 M PB for 2 h followed by washing in PB and incubation in PB with 15% sucrose overnight. The tissue then underwent heat-induced antigen retrieval before blocking with 10% GS in the presence of 0.1% Triton X-100 in PBS for 1 h. To detect  $\alpha_2\delta$ -1, the tissue was incubated with the mouse monoclonal anti- $\alpha_2$ -1 antibody (1:100) in 50% blocking buffer for 48 h at 4°C. After extensive washing with PBS containing 0.1% Triton X-100, the tissue was incubated with biotinylated goat anti-mouse IgG (1:500) for 24 h at 4°C and streptavidin-Alexa Fluor 488 (1:500) for 4 h at RT. After extensive washing and DNA staining with DAPI, samples were mounted in VectaShield (Vector Laboratories).

Experiments were performed on at least two individual rats.

**Image acquisition and analysis.** Immunoperoxidase staining was visualized on a Leica MZ7.5 stereomicroscope with a DC300 camera under transmitted light using the Leica IM50 software (Leica). To quantify  $\alpha_2\delta$ -1 staining in the fasciculus gracilis in saline- or PGB-injected animals, RGB color images were transformed into gray level images using ImageJ software (<http://rsb.info.nih.gov/ij>), and gray level density was measured in a triangular region of interest overlaying the ipsilateral and contralateral side, respectively. Ipsilateral gray level density was then normalized to the contralateral side (=100%). All data are given as the mean  $\pm$  SEM. Statistical significance between SNL plus saline and SNL plus PGB sections was determined with Student's nonpaired *t* test.

To quantify levels of  $\alpha_2\delta$ -1 staining in nonpermeabilized Cos-7 cells, optical sections of 4.1  $\mu$ m thickness with constant photomultiplier settings were acquired midway through the cell in the *z*-axis. Fluorescence density was measured in a region of interest by outlining each individual cell using ImageJ. Fluorescence densities in PGB-treated cells were normalized to the mean value measured in saline-treated control cells. Images of endocytosis of  $\alpha_2\delta$ -1 shown in Figure 6, *I* and *J*, are single 1  $\mu$ m optical sections taken at the level of the flattened plasma membrane of the Cos-7 cells, and therefore the surface immunofluorescence appears as an annulus, rather than a sharply defined ring. To analyze endocytosis, *Z*-stacks with 1  $\mu$ m optical sections were acquired. Regions of interest within cell outlines were defined, and the fluorescence density within this region was measured for each individual excitation channel per section. The amount of protein internalized was defined as the ratio of average fluorescence density in the green channel (labeling procedure as above) and the sum of the average fluorescence densities in the green plus red channels. Results per section were then summarized for each cell.

For the quantitative analysis of fluorescence staining in immunohistochemical sections of DRG cell bodies, at least four nonconsecutive sections (minimum distance, 120  $\mu$ m) were imaged per ganglion. Optical *Z*-stacks of 18 images (optical thickness, 1  $\mu$ m) were acquired sequentially with constant nonsaturated photomultiplier settings. All cells within the visual field were subject to analysis, but only cells with an intact nucleus that was visible at its widest diameter in the stack were actually used. Using ImageJ, stacks were transformed into gray level *Z*-projections and the cell area and mean fluorescence density (FD) [fluorescence intensity in arbitrary units (a.u.) per square micrometer] from two representative regions of interest per cell measured. Fifty to 80 cells per DRG were analyzed. Cells were grouped according to their size (Newton et al., 2001) into three different types: small, <700  $\mu$ m<sup>2</sup>; medium, 700–1100  $\mu$ m<sup>2</sup>; and large, >1100  $\mu$ m<sup>2</sup>. Data are given as the mean  $\pm$  SEM. Statistical significance between the respective ipsilateral and contralateral sides or the ipsilateral sides after different treatments was determined with Student's nonpaired *t* test. Statistical significance between the different size groups within a ganglion was determined with a one-way ANOVA and Bonferroni's post test (GraphPad Prism). On spinal cord sections (optical thickness, >10  $\mu$ m), regions of interest (173  $\times$  588  $\mu$ m) were placed over the ipsilateral and contralateral sides of the dorsal horn to measure fluorescence intensity plot profiles (FI) [gray levels (in arbitrary units) with respect to the distance from the surface (in micrometers)]. The ipsilateral and contralateral profiles were normalized to the maximum value of the contralateral side and the mean plot profile of all sections calculated. Statistical significance was determined with Stu-

dent's nonpaired *t* test [for all statistical tests: \*\*\**p* < 0.001; \*\**p* < 0.01; \**p* < 0.05; not significant (ns), *p* > 0.05].

**Immunoelectron microscopy.** EM detection of  $\alpha_2\delta$ -1 immunoreactivity was performed as previously described using the preembedding immunogold method (Lujan et al., 1996). Briefly, animals were perfused with 4% paraformaldehyde, 0.05% glutaraldehyde, and 15% (v/v) saturated picric acid in 0.1 M PB. Tissue was postfixed overnight, and coronal slices of 60  $\mu$ m thickness were cut on a vibratome. Free-floating sections were blocked in TBS with 10% GS for 1 h at RT and incubated in TBS with 1% GS and anti- $\alpha_2\delta$ -1 antibody at 1:100 for 48 h. After washing with TBS, sections were incubated in TBS with 1% GS and goat anti-mouse IgG coupled to 1.4 nm gold particles (1:100; Nanoprobes) for 3 h. After washing with PBS, sections were postfixed with 1% glutaraldehyde in PBS for 10 min, washed in double-distilled water, followed by a silver enhancement step of the gold particles with a HQ Silver kit (Nanoprobes). Sections were then treated with osmium tetroxide (1% in 0.1 M PB), block-stained with uranyl acetate, dehydrated in a graded series of ethanol, and flat-embedded on glass slides in Durcupan resin (Fluka; Sigma-Aldrich). Regions of interest were cut close to the surface of each block at 70–90 nm on an ultramicrotome (Reichert Ultracut E; Leica) and collected on 200-mesh nickel grids. The regions were stained with 1% aqueous uranyl acetate followed by Reynolds's lead citrate. For controls, primary antibodies were either omitted or replaced with 5% (v/v) normal mouse serum. Under these conditions, no selective labeling was observed. In addition, some sections were incubated with gold-labeled secondary antibodies without silver intensification. This resulted in no metal particles in the sections. Ultrastructural visualization was performed in a Jeol-1010 electron microscope (Jeol). Spinal cord areas were captured at a final magnification of 35,000 $\times$ , whereas images of DRG cell bodies and their axons were acquired at 15,000 $\times$ . Immunogold labeling was quantitatively analyzed on randomly selected 30 ultrathin sections (10 sections/block; three blocks per animal). The density of immunogold particles in dendritic shafts and axon terminals in the spinal cord (particles/100  $\mu$ m<sup>2</sup>) was calculated from an area of  $\sim$ 5000  $\mu$ m<sup>2</sup>. Approximately 1000 immunoparticles were analyzed per condition in DRG cell bodies; immunoparticles were detected in the endoplasmic reticulum (ER) and at the plasma membrane. The ER density (ER particles/100  $\mu$ m<sup>2</sup>) was calculated from randomly selected reference areas of 43  $\mu$ m<sup>2</sup> covering a total of 1287.9  $\mu$ m<sup>2</sup>. In addition, the number of gold particles attached to the plasma membrane (PM particles/100  $\mu$ m) was counted. All DRG somata in the reference area were analyzed. Finally, the density of labeling in DRG axons (particles/100  $\mu$ m<sup>2</sup>) was obtained from reference areas of 43  $\mu$ m<sup>2</sup> covering a total of 1287.9  $\mu$ m<sup>2</sup> per condition.

## Results

### Presynaptic increase of $\alpha_2\delta$ -1 in the superficial and deeper layers of the ipsilateral dorsal horn after SNL

To examine the elevation of  $\alpha_2\delta$ -1 in the dorsal horn after SNL, we first visualized the distribution of  $\alpha_2\delta$ -1 using immunohistochemical methods. The ipsilateral (on the side of ligation)  $\alpha_2\delta$ -1 immunoreactivity in L5 spinal cord sections, at 14 d after ligation, was stronger and extended deeper into the dorsal horn than on the contralateral side (Fig. 1A; supplemental Figs. 1A,B, 2A,B, available at [www.jneurosci.org](http://www.jneurosci.org) as supplemental material). The contralateral  $\alpha_2\delta$ -1 immunoreactivity after SNL (supplemental Fig. 2B, available at [www.jneurosci.org](http://www.jneurosci.org) as supplemental material) showed very similar staining compared with the ipsilateral and contralateral  $\alpha_2\delta$ -1 immunoreactivity in L5 spinal cord sections 14 d after sham surgery (supplemental Fig. 2C,D, available at [www.jneurosci.org](http://www.jneurosci.org) as supplemental material).

To quantify the distribution of  $\alpha_2\delta$ -1 in the dorsal horn, normalized fluorescence intensity profiles of ipsilateral and contralateral superficial and deeper layers from L4–L6 sections were created (Fig. 1B; supplemental Fig. 1C–E, available at [www.jneurosci.org](http://www.jneurosci.org) as supplemental material). Whereas superficial layers receive input from nociceptive DRG neurons, the deeper layers are innervated mainly by non-nociceptive

afferents (Woolf and Fitzgerald, 1986). Compared with the contralateral side at 14 d after SNL, the ipsilateral L5 profile was  $\sim$ 130% higher in the superficial layers of Lissauer's tract and lamina I,  $\sim$ 65% higher in lamina II (at 100  $\mu$ m depth), and still significantly increased in the deeper lamina III at 200  $\mu$ m (Fig. 1B). A similar result was found for ipsilateral L6 profiles at 14 d, and L5 profiles at 7 d after ligation (supplemental Fig. 1C,D, available at [www.jneurosci.org](http://www.jneurosci.org) as supplemental material). In contrast, ipsilateral L5 profiles at 14 d after sham surgery did not differ significantly from the contralateral side, at either 100 or 200  $\mu$ m depth (supplemental Fig. 1E, available at [www.jneurosci.org](http://www.jneurosci.org) as supplemental material). Ipsilateral L4 profiles 14 d after SNL had a  $\sim$ 25% higher level of  $\alpha_2\delta$ -1 immunoreactivity at 100  $\mu$ m depth; however, no difference was seen in lamina III (Fig. 1B, inset). When imaged with constant settings, the ipsilateral and contralateral sides of a L5 spinal cord section, at 14 d after sham surgery, had very similar intensity profiles compared with the contralateral side of a L5 spinal cord section 14 d after SNL (supplemental Fig. 2E, available at [www.jneurosci.org](http://www.jneurosci.org) as supplemental material). This indicates that SNL had no effect on the expression level of  $\alpha_2\delta$ -1 in the contralateral side and that  $\alpha_2\delta$ -1 was only increased in the ipsilateral side after SNL.

We next measured the  $\alpha_2\delta$ -1 mRNA levels in the dorsal horn of L5 spinal cord tissue after SNL. For quantification, the  $\alpha_2\delta$ -1 mRNA level of the ipsilateral and contralateral dorsal horn was normalized to the mRNA levels measured in parallel in contralateral DRGs (=100%). Dorsal horn tissue had a lower  $\alpha_2\delta$ -1 mRNA level than contralateral DRGs, and there was no significant difference between the ipsilateral ( $62 \pm 9\%$ ; *n* = 9) and contralateral side ( $55 \pm 5\%$ ; *n* = 9; *p* = 0.517, nonpaired Student's *t* test), indicating that spinal cord neurons are not the origin of the observed increase of  $\alpha_2\delta$ -1 protein in the dorsal horn.

We performed preembedding immunogold EM on ipsilateral (Fig. 1C,D) and contralateral (Fig. 1E,F) lamina I–III of L4–L6 spinal cord sections to study the subcellular localization of  $\alpha_2\delta$ -1, at 14 d after ligation. Immunogold particles were found throughout all sections at the plasma membrane of presynaptic nerve terminals of DRG neurons (arrowheads), at the plasma membrane of postsynaptic dorsal horn neurons (arrows), and also at intracellular dendritic sites (double arrows). Virtually all the presynaptic  $\alpha_2\delta$ -1 immunoparticles were present on excitatory rather than inhibitory terminals, based on ultrastructural criteria, widely used in the field to distinguish between glutamatergic and GABA/glycinergic axon terminals. These criteria include the presence of round synaptic vesicles in glutamatergic axon terminals and the existence of a postsynaptic density in the postsynaptic element (Fig. 1C–F). Only a single immunoparticle was ever seen over a (presumed inhibitory) terminal with elliptical vesicles and no visible postsynaptic density (data not shown).

Whereas the ratio of presynaptic to postsynaptic labeling in the ipsilateral and contralateral L4 dorsal horn was very similar (Fig. 1G), the presynaptic labeling was markedly increased in the ipsilateral L5 (Fig. 1G) and L6 (data not shown) dorsal horn after SNL. These results show that  $\alpha_2\delta$ -1 is particularly increased in the plasma membrane of presynaptic nerve terminals at the level of ligation. Both nociceptive and non-nociceptive afferents seem to contribute to the elevation, as it is seen both in superficial and in deeper dorsal horn layers.

### Chronic pregabalin alleviates pain behavior and reduces the elevation of $\alpha_2\delta$ -1 in the superficial layers of the ipsilateral dorsal horn

Rats were either injected with PGB or saline for 8 d (30 mg/kg, s.c.; three times per day) starting 1 d after SNL (SNL plus PGB, SNL plus saline). This chronic PGB treatment significantly reduced paw withdrawal frequencies to mechanical and cold stimuli (Fig. 1*H*; supplemental Fig. 3, available at [www.jneurosci.org](http://www.jneurosci.org) as supplemental material) and hence reversed tactile and cold allodynia, both symptoms of ligation-induced neuropathic pain. In SNL plus saline rats, allodynia was present from day 2 after SNL, and was maintained through to day 9, when testing ended. In contrast, chronic PGB treatment resulted in significant reductions in paw withdrawal frequencies, from days 2–9 post-SNL to 2 and 6 g von Frey filaments (Fig. 1*H*; supplemental Fig. 3*A*, available at [www.jneurosci.org](http://www.jneurosci.org) as supplemental material), and from days 4–9 post-SNL to stimulation with the 8 g von Frey filament (supplemental Fig. 3*B*, available at [www.jneurosci.org](http://www.jneurosci.org) as supplemental material). A significant PGB-mediated reduction in response to acetone cooling was observed from day 7 after SNL (supplemental Fig. 3*C*, available at [www.jneurosci.org](http://www.jneurosci.org) as supplemental material). Rotarod testing revealed no sedative side effects or motor impairment of the injection regimen (supplemental Fig. 3*D*, available at [www.jneurosci.org](http://www.jneurosci.org) as supplemental material).

Fluorescence intensity profiles of SNL plus saline or SNL plus PGB L5 spinal cord sections (Fig. 1*I*) showed that, compared with saline injections (blue and black lines), chronic PGB strongly reduced the ipsilateral ligation-mediated  $\alpha_2\delta$ -1 immunofluorescence increase (red line) without affecting the contralateral side (gray line). A significant PGB-mediated reduction was observed in the superficial layers of the dorsal horn at the level of ligation (Fig. 1*I*, inset). For example, in lamina II of L5 and L6 sections, whereas the ipsilateral compared with contralateral  $\alpha_2\delta$ -1 level was increased by ~50 and ~75% after saline injection, this elevation was only ~25 and ~30% after chronic PGB treatment. PGB had no significant effect on  $\alpha_2\delta$ -1 levels in L4 sections (Fig. 1*I*, inset) or in deeper layers of L5/L6 sections (data not shown).

**$\alpha_2\delta$ -1 immunofluorescence is increased in ipsilateral DRG axons of dorsal roots**  
The ligation-mediated ipsilateral  $\alpha_2\delta$ -1 immunofluorescence increase was not re-

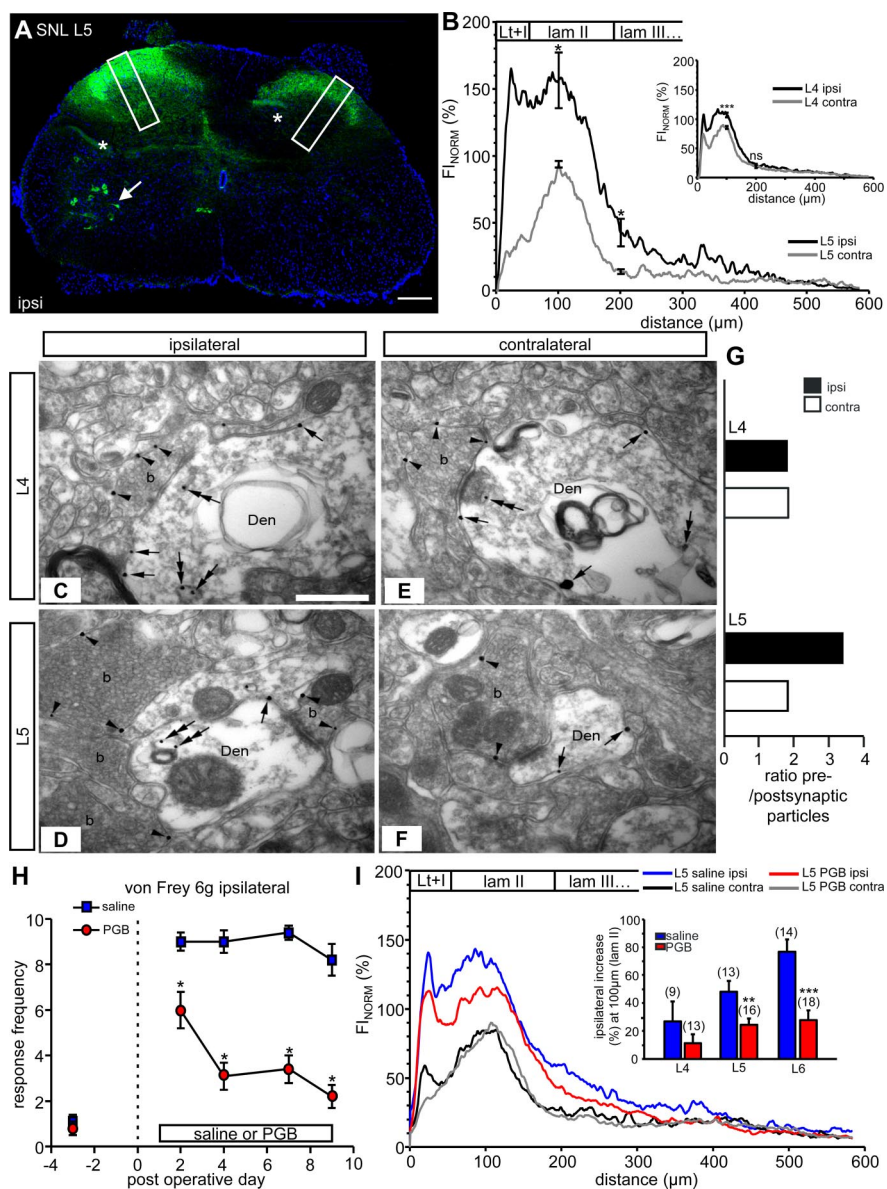


**Figure 1.** Ipsilateral presynaptic increase of  $\alpha_2\delta$ -1 in the superficial and deeper layers of the dorsal horn after L5/L6 SNL is reduced by chronic PGB at a dose that alleviated neuropathic pain. **A**, Representative  $\alpha_2\delta$ -1 immunofluorescence in a montage of 10 images of a transverse L5 spinal cord section 14 d after SNL.  $\alpha_2\delta$ -1 immunofluorescence, Green; nuclear staining, blue; ipsi, ipsilateral side (side of ligation); asterisk (\*), fold in section; rectangles, regions of interest for fluorescence intensity profiles; arrow, ipsilateral motor neurons with elevated  $\alpha_2\delta$ -1 immunofluorescence at the level of ligation. Scale bar, 250  $\mu$ m. **B**, Normalized fluorescence intensity profiles ( $F_{INORM}$ ) of the superficial layers [Lissauer's tract (Lt), lamina I (I), and lamina II (lam II)] and deeper layers (from lamina III onward)] of the ipsilateral (black line) and contralateral (contra) (gray line) L5 ( $n = 4$ ) and L4 (**B**, inset;  $n = 11$ ) dorsal horn 14 d after SNL. Profiles are normalized to the contralateral  $F_{INORM}$  maximum. Error bars represent SEM. For clarity, only error bars at 100  $\mu$ m in lamina II and at 200  $\mu$ m in lamina III are shown. Statistical analysis was as follows: nonpaired Student's *t* test comparing ipsilateral to contralateral side,  $***p < 0.001$ ;  $*p < 0.05$ ; ns (not significant),  $p > 0.5$ . **C–F**, Representative electron micrographs of ipsilateral (**C**, **D**) and contralateral (**E**, **F**) immunogold labeling of  $\alpha_2\delta$ -1 in the dorsal horn (lamina I–III) of L4 and L5 spinal cord sections 14 d after SNL. Scale bar, 0.5  $\mu$ m. Arrowheads, Presynaptic sites at the plasma membrane of excitatory axon terminal boutons (b, characterized by their round synaptic vesicles and opposing postsynaptic density); arrows, postsynaptic sites at the extrasynaptic plasma membrane of dendritic shafts (Den); double arrows, intracellular dendritic sites. For clarity, not all immunoparticles are labeled. **G**, Ratio of presynaptic to postsynaptic number of particles in the ipsilateral (filled bars) and contralateral (open bars) L4 and L5 spinal cord dorsal horn. **H**, Paw withdrawal frequencies to an innocuous mechanical stimulus (von Frey 6 g) applied to the ipsilateral hindpaw of SNL plus saline- (blue squares;  $n = 12$ ) or SNL plus PGB-treated animals (red circles;  $n = 11$ ). Error bars represent SEM. Statistical analysis was as follows: nonparametric Mann–Whitney *U* test,  $*p < 0.05$ . Rats were injected with PGB or saline starting at day 1 after SNL (day 0, dotted line) and killed at day 9. **I**, Normalized fluorescence intensity profiles of ipsi L5 saline- (blue line;  $n = 13$ ), contra L5 saline- (black line;  $n = 13$ ), ipsi L5 PGB- (red line;  $n = 16$ ), and contra L5 PGB-treated (gray line;  $n = 16$ ) dorsal horn regions. **I**, Inset, Ipsilateral  $\alpha_2\delta$ -1 increase compared with contralateral side at 100  $\mu$ m (lam II) in L4–L6 dorsal horn after saline (blue bars) or PGB (red bars) injections. Error bars represent SEM. Statistical analysis was as follows: nonpaired Student's *t* test comparing saline to PGB treatment,  $***p < 0.001$ ;  $**p < 0.01$ . Number of sections is given above bars.

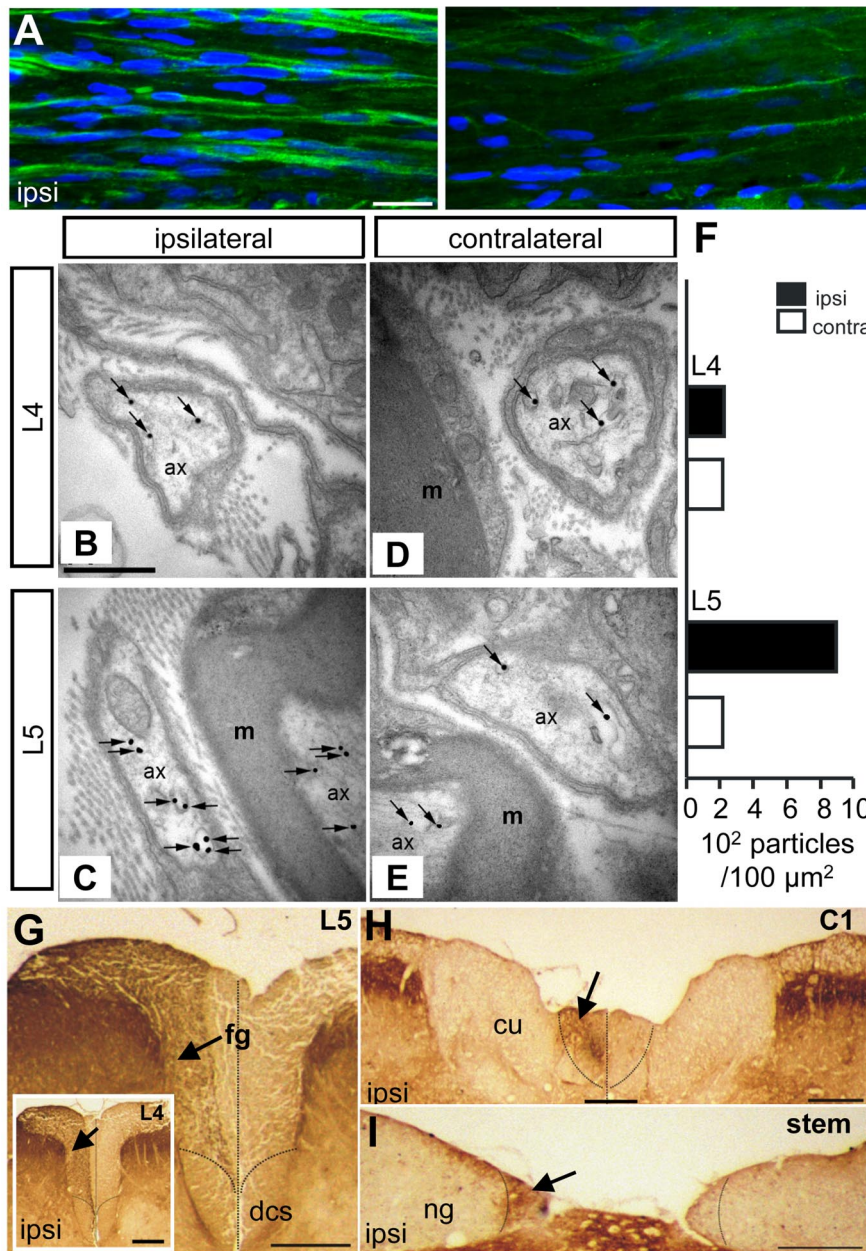


**Figure 2.**  $\alpha_2\delta$ -1 is increased in dorsal roots after SNL and in the ipsilateral ascending tracts from the level of SNL to the brainstem. **A**, Z-projection of 10 optical sections of the ipsilateral (left) and contralateral (right) proximal L5 dorsal root.  $\alpha_2\delta$ -1 immunofluorescence, Green; nuclear staining, blue. Scale bar, 20  $\mu\text{m}$ . **B–E**, Electron micrographs of ipsilateral (**B**, **C**) and contralateral (**D**, **E**) L4 and L5 DRG axons.  $\alpha_2\delta$ -1 immunoparticles at intracellular membranes (arrow) in myelinated (m) and non-myelinated axons (ax). Scale bar, 0.5  $\mu\text{m}$ . **F**, Quantification of immunoparticles ( $10^2$  particles/ $100 \mu\text{m}^2$ ) in ipsilateral (filled bars) and contralateral (open bars) L4 and L5 DRG axons. **G, H**,  $\alpha_2\delta$ -1 immunoperoxidase staining in lumbar L5 (**G**), L4 (**G**, inset), and cervical C1 (**H**) spinal cord sections, 14 d after SNL. **I**,  $\alpha_2\delta$ -1 immunostaining in the brainstem (approximately bregma  $-14.40$ ), 14 d after SNL. Scale bars, 200  $\mu\text{m}$ . Arrows,  $\alpha_2\delta$ -1 staining in the ipsilateral fasciculus gracilis (fg); dcs, dorsal corticospinal tract; cu, cuneate fasciculus; ng, nucleus gracilis.

stricted to the nerve terminals in the spinal cord but was also evident in the axons of DRG neurons in the dorsal root (Fig. 2A). EM analysis showed that the vast majority of  $\alpha_2\delta$ -1 immunoparticles was colocalized with tubulovesicular structures that are involved in protein trafficking, within both myelinated and non-myelinated axons in L4 and L5 spinal nerves (Fig. 2B–E). Immunoparticles at the plasma membrane were rarely observed. L4 axons from SNL animals had a similar number of  $\alpha_2\delta$ -1 immunoparticles on the ipsilateral compared with the contralateral side (Fig. 2B,D; quantified in F). In contrast, after SNL, the im-

munoparticle density in the ipsilateral L5 spinal nerves was markedly increased compared with contralateral axons (Fig. 2C,E; quantified in F). Similar EM results were obtained from L6 spinal nerves (data not shown).

**Chronic pregabalin reduces the elevation of  $\alpha_2\delta$ -1 in the ipsilateral fasciculus gracilis**

As shown in Figure 2G, after SNL, we found substantially more  $\alpha_2\delta$ -1 immunostaining in the ipsilateral L5 fasciculus gracilis (fg, arrow) compared with the contralateral side. The fasciculus gracilis, as part of the dorsal column, contains ascending DRG axons and consequently showed strong  $\alpha_2\delta$ -1 immunoreactivity rostrally from L4 (Fig. 2G, inset) through the cervical C1 region (Fig. 2H) up into the brainstem (Fig. 2I). In contrast, there was no effect of SNL on  $\alpha_2\delta$ -1 immunostaining in the descending dorsal corticospinal tract (dcs) (Fig. 2G).

Chronic PGB significantly reduced the SNL-mediated unilateral  $\alpha_2\delta$ -1 upregulation in the axons of the fasciculus gracilis. When normalized to the contralateral side, the ipsilateral fluorescence density in the fasciculus gracilis in C1 sections after SNL plus saline treatment was  $132 \pm 1\%$  ( $n = 7$ ) compared with  $123 \pm 1\%$  after SNL plus PGB ( $n = 7$ ;  $p = 0.00005$ , nonpaired Student's  $t$  test).

**Upregulation of  $\alpha_2\delta$ -1 mRNA in DRGs after SNL is not affected by chronic PGB**

We wanted to determine whether the effect of PGB was attributable to decreased  $\alpha_2\delta$ -1 transcription or translation in DRGs, or an effect on trafficking. After SNL, the  $\alpha_2\delta$ -1 mRNA level was significantly upregulated by >500% 7 and 14 d after SNL in ligated L5/L6 DRGs, compared with L5/L6 DRGs from sham-operated animals (Fig. 3A). In contrast,  $\alpha_2\delta$ -2 mRNA was significantly downregulated in ipsilateral L5/L6 DRGs by ~70%, at 7 and 14 d after SNL (Fig. 3B). Also,  $\alpha_2\delta$ -3 mRNA was similarly downregulated 14 d after SNL by  $61 \pm 9\%$  ( $n = 4$ ). These results emphasize the dominant role of  $\alpha_2\delta$ -1 over  $\alpha_2\delta$ -2, which also binds gabapentinoid drugs, and  $\alpha_2\delta$ -3, which does not bind these drugs, in the development and treatment of neuropathic pain. In contrast, the mRNA levels for  $\alpha_2\delta$ -1,  $\alpha_2\delta$ -2, and  $\alpha_2\delta$ -3 were not significantly changed in ipsilateral L4 DRGs from SNL- and sham-operated animals (supplemental Fig. 4A, available at www.jneurosci.org as supplemental material) (data not shown).

To investigate the mode of action of chronic PGB, we examined  $\alpha_2\delta$ -1 mRNA levels in L5/L6 DRGs from SNL plus saline and SNL plus PGB-treated animals. We found that the ipsilateral  $\alpha_2\delta$ -1 mRNA level was also significantly upregulated by >500%

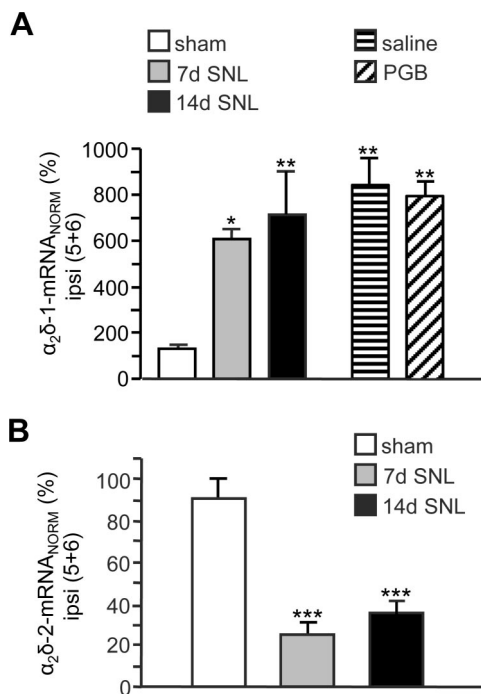


**Figure 3.** Upregulation of  $\alpha_2\delta$ -1 mRNA after SNL is not affected by chronic PGB. **A**, Q-PCR results for  $\alpha_2\delta$ -1 mRNA levels (percentage) in pooled ipsilateral L5/L6 DRGs (ipsi 5 + 6) from sham-operated animals (open bars;  $n = 5$ ), from animals 7 d ( $n = 4$ ; gray bars) or 14 d ( $n = 7$ ; black bars) after SNL and from SNL plus saline (horizontal striped bar;  $n = 4$ ) or SNL plus PGB animals (hatched bar;  $n = 4$ ). Data are normalized to the respective contralateral side. Error bars represent SEM. Statistical analysis was as follows: one-way ANOVA with  $p = 0.0031$  using SNK post test; \*\*\* $p < 0.01$ ; \* $p < 0.05$ . Note: Increase in SNL plus PGB animals was not significantly different from SNL plus saline animals in SNK post test ( $p > 0.05$ ). **B**, Q-PCR results for  $\alpha_2\delta$ -2 mRNA levels (percentage) in pooled ipsilateral L5/L6 DRGs (ipsi 5 + 6) from either sham-operated animals (open bars;  $n = 5$ ) or from animals 7 d ( $n = 4$ ; gray bars) or 14 d ( $n = 7$ ; black bars) after SNL. Data are normalized to the respective contralateral side. Error bars represent SEM. Statistical analysis was as follows: one-way ANOVA with  $p < 0.0001$  using SNK post test, \*\*\* $p < 0.001$ .

in SNL plus saline animals (Fig. 3A). Chronic PGB had no effect on this elevation (Fig. 3A), indicating that the gene expression of  $\alpha_2\delta$ -1 was not affected.

**Upregulation of  $\alpha_2\delta$ -1 in all size groups of DRG somata after SNL is mainly intracellular and is not affected by chronic PGB**  
The ipsilateral ligation-mediated increase of  $\alpha_2\delta$ -1 mRNA was reflected in a  $\sim 10$ -fold increase of  $\alpha_2\delta$ -1 protein in L5/L6 DRGs compared with contralateral L4–L6 and ipsilateral L4 DRGs as measured by Western blotting (supplemental Fig. 4B, available at www.jneurosci.org as supplemental material). In contrast,  $\alpha_2\delta$ -2 protein was not detectable (data not shown).

At the cellular level, DRG somata, characterized by dimly stained large nuclei, exhibited a wide range of positive  $\alpha_2\delta$ -1 immunofluorescence, whereas satellite cells with brightly stained smaller nuclei did not show  $\alpha_2\delta$ -1 immunofluorescence (Fig. 4A; supplemental Figs. 4C, 5A, available at www.jneurosci.org as supplemental material). After SNL, the  $\alpha_2\delta$ -1 immunoreactivity was significantly increased in all ipsilateral L5 (Fig. 4A, left panel) (quantified in Fig. 4B) and L6 (data not shown) somata, independent of their size. DRG neurons with small and medium-sized somata are mainly nociceptors, whereas non-nociceptive neurons have a large soma (Newton et al., 2001). In addition to the  $\alpha_2\delta$ -1 increase at the level of ligation, in ipsilateral L4, 13% of small somata were significantly brighter than the contralateral maximum fluorescence density (supplemental Fig.

4C,D, available at www.jneurosci.org as supplemental material). However, this effect was a result of the surgery, rather than the ligation, since 23% of small ipsilateral L4 DRG somata from sham-operated animals showed a similar increase in  $\alpha_2\delta$ -1 immunofluorescence (supplemental Fig. 5A,B, available at www.jneurosci.org as supplemental material).

EM images from ipsilateral and contralateral L4 and L5 DRGs from SNL rats show that  $\alpha_2\delta$ -1 was mainly associated with the ER (Fig. 4C–J, arrows). However, it was also present at the PM (Fig. 4E,F,I,J, arrowheads). Whereas the number of immunoparticles associated with the ER or PM was similar on the ipsilateral and contralateral side in L4 cell bodies (Fig. 4K), in L5, both the ipsilateral ER and PM localization was increased approximately fourfold over the contralateral side after SNL (Fig. 4L). Similar results were obtained from electron micrographs of L6 DRG cell bodies (data not shown).

Compared with SNL plus saline, PGB had no significant effect on the level of  $\alpha_2\delta$ -1 immunofluorescence measured in small, medium, and large L5 DRG neurons after SNL (Fig. 4M,N), indicating that it did not alter the somatic  $\alpha_2\delta$ -1 protein levels of either nociceptors or non-nociceptors.

### Proximal accumulation of $\alpha_2\delta$ -1 at the ligation site demonstrates anterograde trafficking

Images from dorsal root regions 2, 4, and 7 d after SNL (Fig. 5A,B) show a gradual increase of the ipsilateral  $\alpha_2\delta$ -1 immunofluorescence with time indicating increased trafficking of  $\alpha_2\delta$ -1 protein from the DRG cell body along the axons.

A well established method to determine the direction of axonal protein trafficking is to perturb the trafficking by nerve ligation causing the protein to accumulate at the ligation site. As shown in Figure 5C, there was a much stronger immunofluorescence staining of  $\alpha_2\delta$ -1 at the proximal compared with the distal side 4 d after SNL. A similar accumulation of  $\alpha_2\delta$ -1 was observed 2 d after ligation (data not shown). This indicates that  $\alpha_2\delta$ -1 was trafficked anterogradely originating from the DRG cell bodies. The gradual accumulation of  $\alpha_2\delta$ -1 along the spinal nerve toward the ligation site (Fig. 5C) was absent on the nonligated contralateral side (Fig. 5D). The proximal accumulation of  $\alpha_2\delta$ -1 was confirmed by immunoblotting of proteins extracted from ipsilateral L5 spinal nerve, dorsal root segments and DRGs 4 d after SNL (Fig. 5E). For quantification, spinal nerve and dorsal root protein levels were normalized to the level of  $\alpha_2\delta$ -1 protein detected in DRGs (= 100%) (Fig. 5F, lane 5). SNL caused  $\alpha_2\delta$ -1 to accumulate at the proximal ligation site to a similar level to that found in DRGs (Fig. 5F, lane 3) ( $100 \pm 8\%$ ;  $n = 8$ ), whereas at the distal ligation site the level of  $\alpha_2\delta$ -1 protein was much lower (only  $35 \pm 15\%$  of the DRG protein level) (Fig. 5F, lane 2). The  $\alpha_2\delta$ -1 protein in DRGs had a slightly higher molecular weight than the trafficked protein detected in the adjacent spinal nerves and dorsal roots. A similar difference in the molecular weight between  $\alpha_2\delta$ -1 protein in DRGs and  $\alpha_2\delta$ -1 isolated from spinal cord tissue was previously identified as a difference in protein glycosylation (Luo et al., 2001). Chronic application of PGB for 3.5 d reduced the accumulation of  $\alpha_2\delta$ -1 at the site proximal to the ligation of the spinal nerve compared with the accumulation in saline-injected animals. We found that, after PGB injections, the  $\alpha_2\delta$ -1 protein level at the proximal ligation site was reduced by 24 and 32% compared with saline-injected animals (tissue pooled from two to four animals processed in two independent experiments).

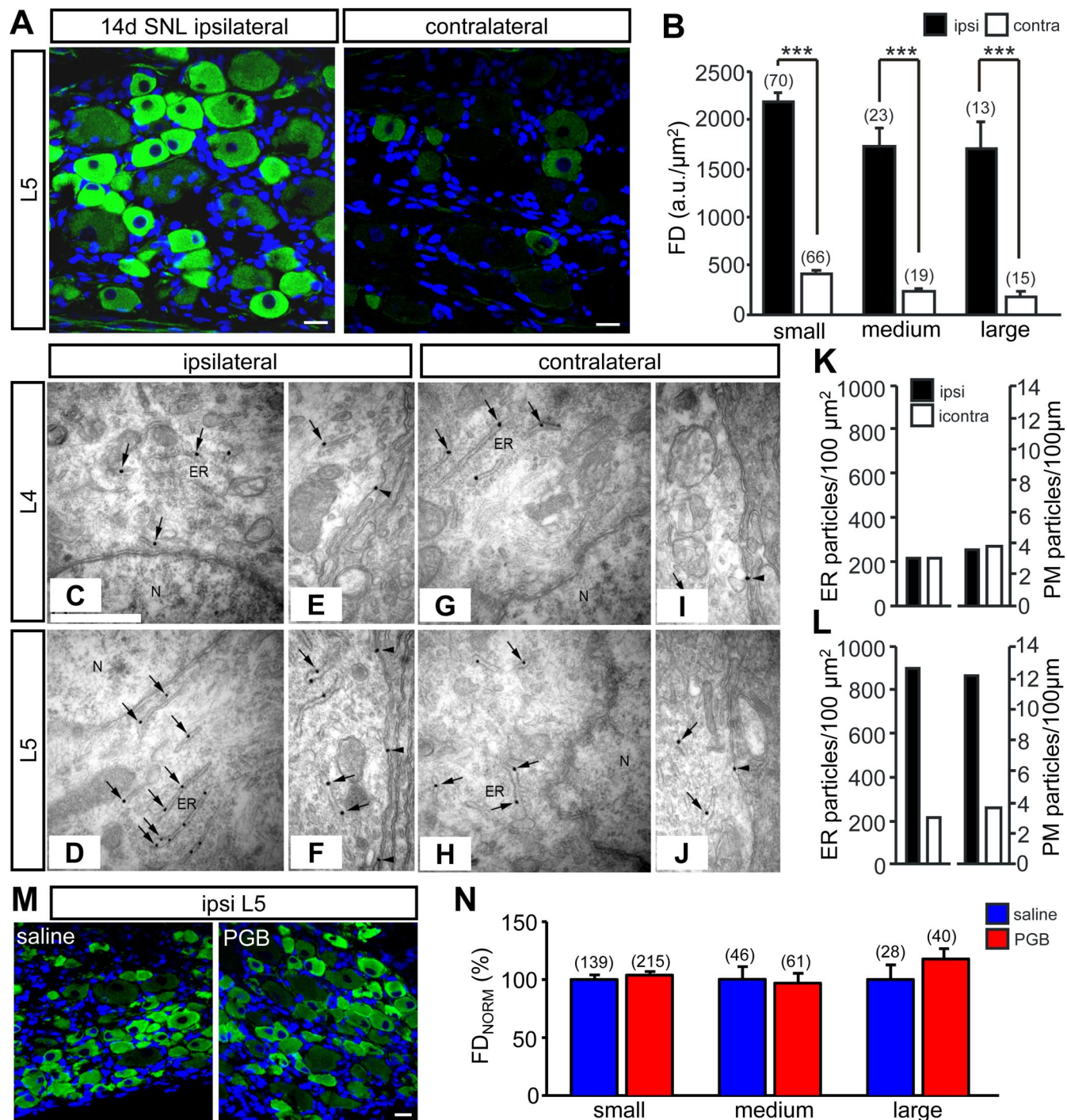


**Figure 4.** SNL-mediated ipsilateral increase of  $\alpha_2\delta$ -1 protein levels in DRG somata is not affected by chronic PGB. **A**, Single images of ipsilateral (left) and contralateral (right) L5 DRG sections 14 d after ligation.  $\alpha_2\delta$ -1 Immunofluorescence, Green; nuclear staining, blue. Scale bar, 20  $\mu\text{m}$ . **B**, Mean intracellular FD [in arbitrary units (a.u.) per square micrometer] of ipsilateral (filled bars) and contralateral (open bars) small (<700  $\mu\text{m}^2$ ), medium (700–1100  $\mu\text{m}^2$ ), and large (>1100  $\mu\text{m}^2$ ) DRG somata 14 d after SNL. Error bars represent SEM. Statistical analysis was as follows: nonpaired Student's *t* test comparing ipsilateral to contralateral side, \*\*\**p* < 0.001. Numbers of cells are given above bars. **C–J**, Electron micrographs of ipsilateral L4 (**C**) and L5 (**D**) DRG somata adjacent to the nucleus (N) and PM [**E**]; L5 (**F**)] 14 d after ligation. Immunoparticles for  $\alpha_2\delta$ -1 are mainly associated with the ER (arrows) and also at PM (arrowheads). Micrographs of contralateral L4 (**G**) and L5 (**H**) DRG somata and PM [L4 (**I**); L5 (**J**)]. Scale bar, 0.5  $\mu\text{m}$ . For clarity, not all immunoparticles are labeled. **K, L**, Quantification of immunoparticle density in the ER (particles/100  $\mu\text{m}^2$ ; left) and number of particles at the PM (particles/100  $\mu\text{m}$ ; right) in ipsilateral (filled bars) and contralateral (open bars) L4 and L5 DRG somata. **M**, Images of ipsilateral L5 DRG sections from SNL plus saline or SNL plus PGB animals.  $\alpha_2\delta$ -1 Immunofluorescence, Green; nuclear staining, blue. Scale bar, 20  $\mu\text{m}$ . **N**, Normalized fluorescence density (FD<sub>NORM</sub>) of ipsilateral small, medium, and large DRG somata after SNL plus saline (blue bars) or SNL plus PGB treatment (red bars). Data are normalized to mean FD of respective SNL plus saline size group. Error bars represent SEM. Statistical analysis was as follows: nonpaired Student's *t* test comparing saline to PGB treatment, *p* = 0.417 for small; *p* = 0.801 for medium; *p* = 0.223 for large cell bodies. Numbers of cells analyzed are given above bars.

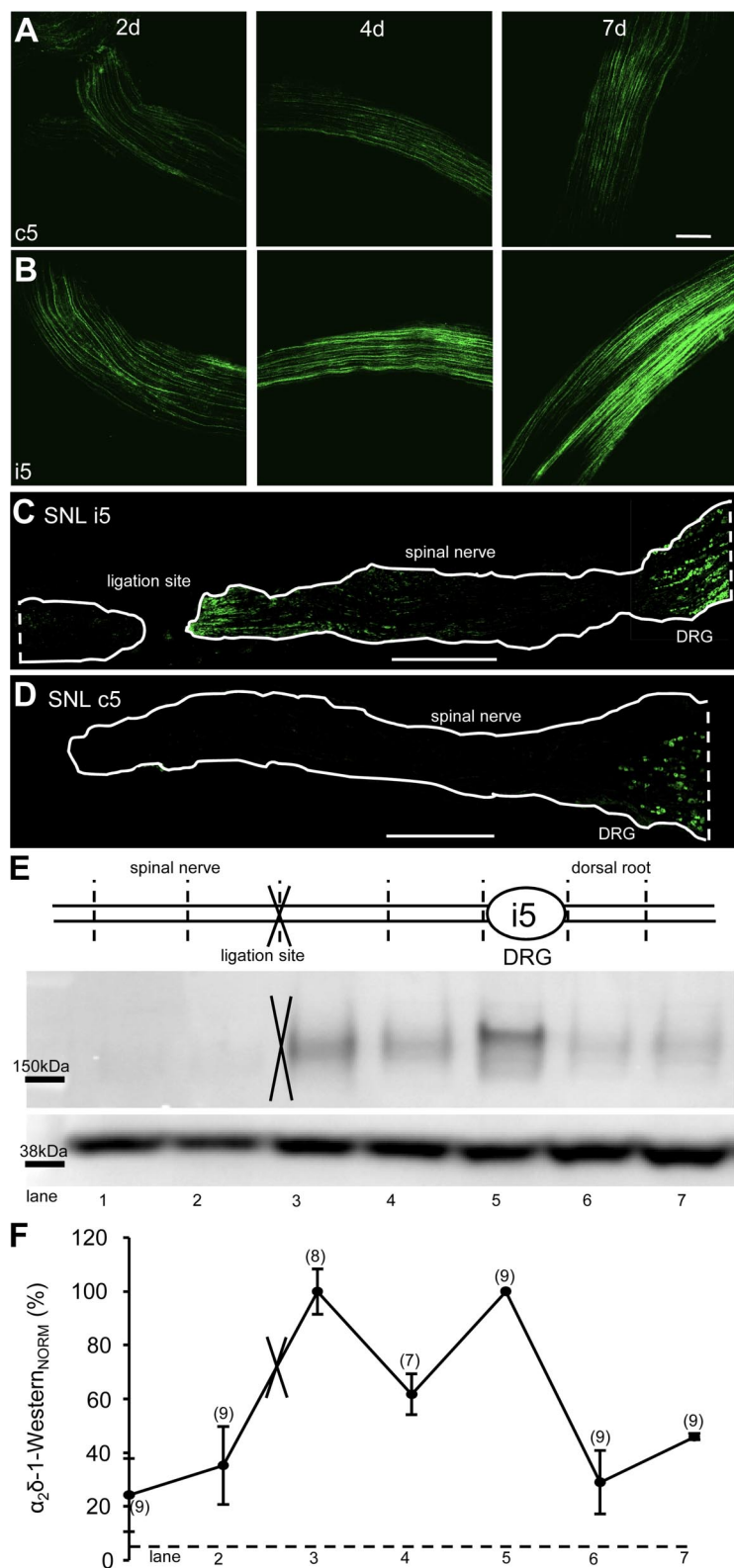


**Figure 5.** Increase of  $\alpha_2\delta$ -1 protein with time in dorsal roots and accumulation proximal to the ligation site. **A**, Representative single images of contralateral L5 dorsal roots 2 d (left), 4 d (middle), and 7 d after SNL (right). **B**, Representative single images of ipsilateral L5 dorsal roots 2 d (left), 4 d (middle), and 7 d after SNL.  $\alpha_2\delta$ -1 Immunofluorescence, Green. Scale bar, 200  $\mu$ m. **C**, Single image of an ipsilateral L5 spinal nerve and DRG section 4 d after ligation.  $\alpha_2\delta$ -1 Immunofluorescence, Green; outline, white; tissue boundaries determined with nuclear staining (data not shown). Scale bar, 1 mm. **D**, Single image of a contralateral L5 spinal nerve and DRG section 4 d after ligation.  $\alpha_2\delta$ -1 Immunofluorescence, Green; outline, white; tissue boundaries determined with nuclear staining (data not shown). Scale bar, 1 mm. Note: Stronger  $\alpha_2\delta$ -1 staining in the ipsilateral DRG neuron somata compared with the contralateral side. **E**, Top, Diagram of ipsilateral L5 spinal nerve showing ligation site, DRG, and dorsal root segments used for Western blotting. Middle, Representative immunoblot of  $\alpha_2\delta$ -1 expression in spinal nerve segments

### Pregabalin reduces the $\alpha_2\delta$ -1 level at the plasma membrane without affecting endocytosis

We next probed *in vitro* the mechanism of action of PGB, by examining whether PGB caused a reduction of  $\alpha_2\delta$ -1 trafficking as determined by expression at the plasma membrane. First, we characterized the properties of the anti- $\alpha_2\delta$ -1 antibody used for this purpose. Figure 6A shows a representative image of the intracellular distribution of  $\alpha_2\delta$ -1 in transfected and permeabilized Cos-7 cells (green staining) also expressing  $Ca_v2.2$  and  $\beta 1b$  to mimic the native calcium channel composition found in DRGs. In nonpermeabilized cells (Fig. 6B),  $\alpha_2\delta$ -1 is detected in the plasma membrane indicating that the antibody recognizes an extracellular epitope of  $\alpha_2\delta$ -1. To confirm the specificity of the antibody, cells simultaneously probed with anti- $\alpha_2\delta$ -2 (red) and anti- $\alpha_2\delta$ -1 antibody while expressing  $\alpha_2\delta$ -2 (Fig. 6C) showed only  $\alpha_2\delta$ -2 staining. As shown in Figure 6D–F, cell surface expression of  $\alpha_2\delta$ -1 was measured in nonpermeabilized Cos-7 cells. Omission of the primary antibody served as a negative control (Fig. 6G). Application of 20 or 200  $\mu$ M PGB, for 72 h after transfection, reduced plasma membrane immunofluorescence of  $\alpha_2\delta$ -1 (Fig. 6E,F) by  $\sim 40$  and  $\sim 65\%$ , respectively (Fig. 6H), when compared with saline-treated control cells (Fig. 6D,H).

Although this result agrees with our *in vivo* findings in the spinal cord (Fig. 1I), both could, in principle, be attributable either to a reduction of anterograde trafficking or to an increase in endocytosis of  $\alpha_2\delta$ -1 subunits by PGB. To examine a possible effect of chronic PGB on endocytosis, nonpermeabilized living Cos-7 cells expressing  $\alpha_2\delta$ -1 (together with  $Ca_v2.2$  and  $\beta 1b$ ) were incubated at 72 h posttransfection with  $\alpha_2\delta$ -1 antibody at 37°C for 2.5 h, allowing endocytosis to occur. They were then fixed and all remaining cell surface  $\alpha_2\delta$ -1 was saturated with a secondary antibody (red). After permeabilization, endocytosed  $\alpha_2\delta$ -1 was then labeled (Fig. 6I,J, green). To quantify endocytosis, the

(lanes 1–4 with ligation site marked with X between lanes 2 and 3), DRG (lane 5), and dorsal root segments (lane 6 and 7) pooled from four animals 4 d after ligation. Bottom, Corresponding immunoblot of GAPDH expression in ipsilateral L5 spinal nerve, DRG, and dorsal root tissue. **F**, Quantification of three immunoblots of  $\alpha_2\delta$ -1 expression in pooled spinal nerve and dorsal root segments 4 d after SNL corrected for gel loading (GAPDH protein level) and normalized to the  $\alpha_2\delta$ -1 level in the DRGs (number of tissue segments in parentheses). Error bars represent SEM.

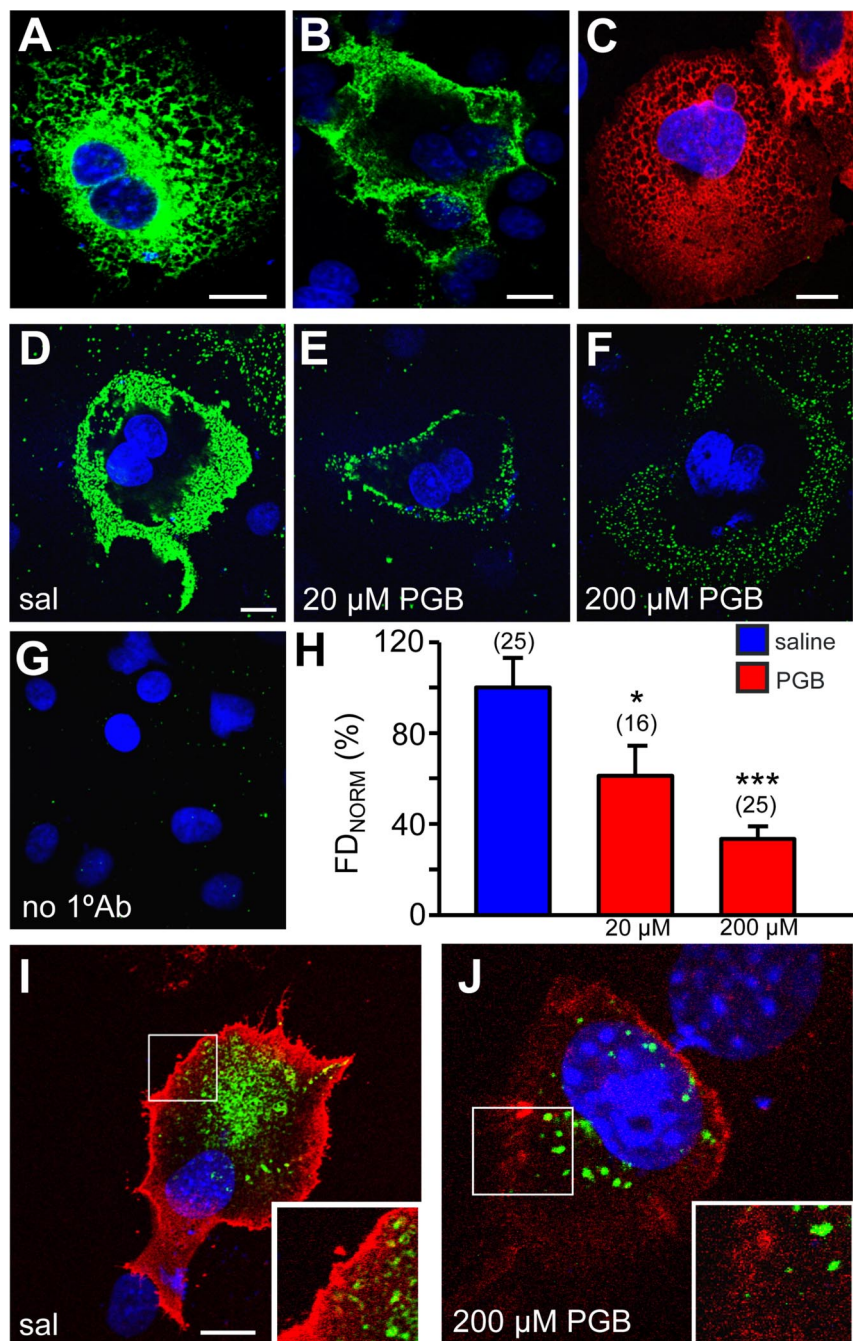


**Figure 6.** PGB reduces cell surface expression but does not affect endocytosis of  $\alpha_2\delta$ -1. **A–C**, Localization of exogenous  $\alpha_2\delta$ -1 in Cos-7 cells that were either permeabilized (**A**) or nonpermeabilized (**B**) before immunostaining with anti- $\alpha_2\delta$ -1 antibody (green). **C**, Staining for exogenous  $\alpha_2\delta$ -2 in permeabilized Cos-7 cells with anti- $\alpha_2\delta$ -2 antibody (red) in presence of the anti- $\alpha_2\delta$ -1 antibody (green). Nuclear staining, Blue. Note: Lack of green staining indicates lack of cross-reactivity of the anti- $\alpha_2\delta$ -1 antibody. Scale bar, 20  $\mu$ m. **D–F**, Images of surface expression of  $\alpha_2\delta$ -1 (green) in nonpermeabilized Cos-7 cells treated with 0 (saline; **D**), 20 (**E**) or 200 (**F**)  $\mu$ M PGB for 72 h. **G**, No primary antibody. Nuclear staining, Blue. Scale bar, 20  $\mu$ m. **H**, Normalized fluorescence densities (FD<sub>NORM</sub>) after saline (blue bar) and 20 or 200  $\mu$ M PGB treatment (red bars). FDs were normalized to the mean FD of saline-treated cells. Error bars represent SEM. Statistical analysis was as follows: one-way ANOVA,  $p < 0.0001$ , with Bonferroni's post test,  $*p < 0.05$  and  $***p < 0.001$ . Number of cells examined is given above bars. **I, J**, Images of  $\alpha_2\delta$ -1 endocytosis assay in Cos-7 cells performed in absence (saline; **I**) or presence of 200  $\mu$ M PGB (**J**). Cell surface  $\alpha_2\delta$ -1, Red; internalized  $\alpha_2\delta$ -1, green; nuclear staining, blue. Scale bar, 20  $\mu$ m.

ratio of internal fluorescence density/total fluorescence density was calculated. In control cells (saline-treated;  $n = 20$ ),  $15 \pm 2\%$  of  $\alpha_2\delta$ -1 was endocytosed in 2.5 h, indicating that  $\alpha_2\delta$ -1 is subject to constitutive endocytosis. However, when PGB (200  $\mu$ M) was present in the medium from the time of transfection and during

the endocytosis period, it had no significant effect on the amount of constitutive endocytosis ( $20 \pm 4\%$ ;  $n = 20$ ;  $p = 0.2187$ , nonpaired Student's  $t$  test). Essentially the same results were obtained using  $\alpha_2\delta$ -2 and up to 1 mM gabapentin (data not shown), reinforcing the view that the gabapentinoid  $\alpha_2\delta$  ligands do not act by enhancing endocytosis of calcium channels.

## Discussion

Our data provide a possible explanation of how chronic application of PGB can alleviate neuropathic pain by reducing anterograde trafficking and consequently reducing the level of presynaptic  $\alpha_2\delta$ -1 in nerve terminals in the spinal cord.

After SNL, we found that the elevation of  $\alpha_2\delta$ -1 protein in DRGs occurs throughout the cytoplasm in all DRG cell subtypes, as also shown for  $\alpha_2\delta$ -1 mRNA after partial sciatic nerve injury (Newton et al., 2001) and in diabetic neuropathy (Yusaf et al., 2001). However, in contrast to mRNA levels, the detection and quantification of  $\alpha_2\delta$ -1 protein provides a more functional assessment. Previous studies have shown an upregulation of  $\alpha_2\delta$ -1 protein in DRGs and spinal cord using immunoblotting or  $^3$ H-gabapentinoid binding, but those approaches lack cellular and subcellular resolution (Luo et al., 2001; Field et al., 2006; Melrose et al., 2007). Using immunohistochemistry, we were able to detect small changes in subpopulations of cells that would be undetectable by other methods. Moreover, our ultrastructural analysis enabled us to determine the subcellular localization of upregulated  $\alpha_2\delta$ -1 protein in DRG somata and axons as mainly intracellular, being mainly within the ER in cell bodies and associated with tubular-vesicular structures involved in protein trafficking in the dorsal root.

The upregulation of  $\alpha_2\delta$ -1 in the spinal cord is critical for the initiation and maintenance of neuropathic pain (Boroujerdi et al., 2008). We found a highly significant presynaptic increase of  $\alpha_2\delta$ -1 in the nerve terminals of DRG neurons that innervate the superficial and deeper layers of the dorsal horn. Almost no  $\alpha_2\delta$ -1 immunoparticles were observed to be associated with inhibitory terminals, and this labeling was not increased after SNL. Moreover, there was no increase in  $\alpha_2\delta$ -1 mRNA in dorsal horn neurons within the spinal cord after SNL. Therefore, our EM and quantitative RT-PCR results are the first direct evidence that the  $\alpha_2\delta$ -1 elevation after SNL occurs exclusively in presynaptic terminals of primary sensory afferents, whereas previous studies have relied on more indirect methods to interpret the increase of  $\alpha_2\delta$ -1 in the

dorsal horn (Wang et al., 2002; Li et al., 2004). The majority of unmyelinated nociceptive primary afferents synapse mainly in lamina I and II of the dorsal horn within the same spinal segment. However, a proportion of afferents project in Lissauer's tract to up to two spinal segments rostrally and one spinal segment caudally. The L4 dorsal horn not only receives afferents from L4, but also from ligated L5/L6 dorsal roots (Besse et al., 1991; Shehab et al., 2008). This may contribute to the small, but statistically significant elevation of  $\alpha_2\delta$ -1 in ipsilateral L4 after SNL.

Small-diameter, unmyelinated C-fibers convey thermal hyperalgesia, whereas tactile allodynia is transmitted mainly through large-diameter A $\beta$  afferent fibers (Sun et al., 2001; Pitcher and Henry, 2004). As well as terminating in deeper layers of the dorsal horn, some myelinated medium and large DRG neurons, involved in touch and proprioception, send their axons to the brainstem via the fasciculus gracilis in the dorsal column. Furthermore, ablation of the ipsilateral dorsal column in SNL rats blocks tactile allodynia (Sun et al., 2001). Accordingly, we found that  $\alpha_2\delta$ -1 immunoreactivity was elevated unilaterally in this ascending tract, at all levels above the ligation, in agreement with our finding that  $\alpha_2\delta$ -1 is elevated in all DRG cell subtypes. Tactile allodynia may be linked to increased activity in this ascending pathway to supraspinal sites (Sun et al., 2001), whereas thermal hyperalgesia may be mediated through local spinal circuitry (Miki et al., 2000).

Spinal voltage-gated calcium channels are important targets in the treatment of pain (Snutch, 2005). Upregulation of  $\alpha_2\delta$ -1 in the spinal cord is thought to increase presynaptic Ca<sup>2+</sup> influx and neurotransmitter release, therefore sensitizing the spinal cord, an important component of neuropathic pain. Furthermore, the ability of the  $\alpha_2\delta$  ligand drugs to alleviate neuropathic pain is thought to be causally related to the elevation of  $\alpha_2\delta$ -1 in injured DRGs after nerve ligation (for review, see Cheng and Chiou, 2006). In several neuropathic pain models, gabapentin was able to reduce transmitter release or excitatory synaptic transmission in the spinal cord (Patel et al., 2000; Coderre et al., 2005). However, in other studies in naive animals, either no acute effects of gabapentin were found on spontaneous synaptic currents in lamina II neurons (Moore et al., 2002), or gabapentin reduced both inhibitory and excitatory transmission in the mouse spinal cord dorsal horn through a preferential block only of P/Q-type Ca<sup>2+</sup> channels (Bayer et al., 2004). Therefore, the mode of action of gabapentin is still under debate. A key finding of this study is that the ipsilateral presynaptic elevation of  $\alpha_2\delta$ -1 in the dorsal horn after SNL was very substantially and significantly reduced by chronic PGB, at a dose sufficient to reverse the behavioral manifestations of SNL. Furthermore, there was also less elevation of  $\alpha_2\delta$ -1 in the ipsilateral axons of the fasciculus gracilis, an observation that may be relevant to explain the antiallodynic effect of PGB.

In contrast, we found no effect of chronic PGB treatment on  $\alpha_2\delta$ -1 mRNA and protein levels in DRG cell bodies. This indicates that it is not the expression of  $\alpha_2\delta$ -1, but its trafficking from the DRG cell bodies to the presynaptic terminals that is affected by PGB. However, our finding that  $\alpha_2\delta$ -2 and  $\alpha_2\delta$ -3 mRNA are substantially downregulated in SNL suggests that  $\alpha_2\delta$ -1 may also substitute for these species in SNL, potentially increasing the sensitivity to gabapentinoid drugs.

Acute inhibitory effects of gabapentinoid drugs on transmitter release and synaptic transmission have been observed in some, but not all *in vitro* systems (for review, see Davies et al., 2007). For example, in the trigeminal nucleus, an effect of gabapentin was only observed on a component of transmitter release that was

enhanced after protein kinase C activation (Maneuf and McKnight, 2001). Related to this, it has been shown that calcium channel insertion into the plasma membrane is enhanced by protein kinase C activation (Zhang et al., 2008).

In all behavioral measures of tactile allodynia presented here, there was an increasing antiallodynic effect of PGB over the period of treatment. Cold allodynia was only significantly attenuated after 7 d of PGB administration. Although the behavioral therapeutic effects of gabapentinoid drugs are often observed acutely (Field et al., 2006), this is not always the case (Hao et al., 2000; Fox et al., 2003; Xiao et al., 2007). It has also been shown that gabapentin is ineffective acutely if administered after, rather than before, a traumatic insult, such as intraplantar formalin injection (Yoon and Yaksh, 1999). This has been interpreted as gabapentin preventing the initiation of an upregulated persistent pain state, which would translate in the patient to an antihyperalgesic action of this drug occurring after a delay, whose duration would depend on the nature of the persistent injury and the rate of turnover of the "facilitatory cascade" associated with the pain state (Yoon and Yaksh, 1999). Consequently, it is possible that these drugs have acute effects on synaptic transmission under certain conditions, as well as the effects described here to counter the SNL-induced elevation of  $\alpha_2\delta$ -1 in injured DRG axons and presynaptic terminals. Indeed, facilitatory spinal cord–brain–spinal cord circuits (Suzuki et al., 2004) have been shown to rapidly induce a permissive state-dependency for gabapentin in naive animals, through a descending facilitatory spinal 5-hydroxytryptamine receptor-mediated pathway, that could mediate the fast-onset effects of  $\alpha_2\delta$  ligands (Suzuki et al., 2005). One can envisage a scenario after SNL, whereby both the elevation of presynaptic  $\alpha_2\delta$ -1 and the release of mediators in the dorsal horn (for review, see Svensson and Yaksh, 2002) exercise a concerted effect to increase calcium channel insertion into presynaptic terminals and to enhance transmitter release. Thus, gabapentinoid drugs might act more or less rapidly depending on the interplay between these different elements.

Chronic PGB application dramatically reduced the cell surface expression of  $\alpha_2\delta$ -1 *in vitro* without affecting constitutive endocytosis. The observed constitutive endocytosis agrees with the relatively high proportion of postsynaptic  $\alpha_2\delta$ -1 in the spinal cord electron micrographs that was present in intracellular vesicles. Related to this, we have shown that both  $\alpha_2\delta$ -1 and  $\alpha_2\delta$ -2 are present in cholesterol-rich lipid raft fractions (Davies et al., 2006), which are associated with the endocytotic machinery (Glebov et al., 2006).

Our recent work has suggested that  $\alpha_2\delta$  subunits have an effect on calcium channel trafficking via the Von Willebrand factor-A domain in the  $\alpha_2$  subunit (Cantí et al., 2005), and furthermore, gabapentinoid drugs exert their effects intracellularly to disrupt the process of  $\alpha_2\delta$  trafficking (Hendrich et al., 2008). In that study, because of the reduced trafficking shown by the mutant R217A- $\alpha_2\delta$ -1 and R282A- $\alpha_2\delta$ -2, which do not bind gabapentin, we speculated that these drugs may displace an endogenous small molecule ligand that might be important for correct trafficking of these  $\alpha_2\delta$  subunits (Heblich et al., 2008; Hendrich et al., 2008). Little is known about the trafficking of  $\alpha_2\delta$ -1, and indeed the images of  $\alpha_2\delta$ -1 accumulation proximal to the ligation site and the localization in axonal tubulovesicular structures represent the first direct evidence for  $\alpha_2\delta$ -1 trafficking.

In conclusion, this study supports the hypothesis that  $\alpha_2\delta$ -1 subunits are involved in trafficking of calcium channels from the site of synthesis to the plasma membrane of the presynaptic terminals. Both our *in vivo* and *in vitro* data point to the gabapentin-

oid drugs inhibiting this process in neuropathic pain, making this a unique mode of action, contrasting with the direct cell surface effects of other drugs used in this condition.

## References

- Barclay J, Balaguero N, Mione M, Ackerman SL, Letts VA, Brodbeck J, Canti C, Meir A, Page KM, Kusumi K, Perez-Reyes E, Lander ES, Frankel WN, Gardiner RM, Dolphin AC, Rees M (2001) Ducky mouse phenotype of epilepsy and ataxia is associated with mutations in the *Cacna2d2* gene and decreased calcium channel current in cerebellar Purkinje cells. *J Neurosci* 21:6095–6104.
- Bayer K, Ahmadi S, Zeilhofer HU (2004) Gabapentin may inhibit synaptic transmission in the mouse spinal cord dorsal horn through a preferential block of P/Q-type  $\text{Ca}^{2+}$  channels. *Neuropharmacology* 46:743–749.
- Bennett GJ, Chung JM, Honore M, Seltzer Z (2003) Models of neuropathic pain in the rat. *Curr Protoc Neurosci* 9:9.14.
- Besse D, Lombard MC, Besson JM (1991) The distribution of  $\mu$  and  $\delta$  opioid binding sites belonging to a single cervical dorsal root in the superficial dorsal horn of the rat spinal cord: a quantitative autoradiographic study. *Eur J Neurosci* 3:1343–1352.
- Boroujerdi A, Kim HK, Lyu YS, Kim DS, Figueroa KW, Chung JM, Luo ZD (2008) Injury discharges regulate calcium channel  $\alpha_2\delta$ -1 subunit upregulation in the dorsal horn that contributes to initiation of neuropathic pain. *Pain* 139:358–366.
- Brodbeck J, Davies A, Courtney JM, Meir A, Balaguero N, Canti C, Moss FJ, Page KM, Pratt WS, Hunt SP, Barclay J, Rees M, Dolphin AC (2002) The ducky mutation in *Cacna2d2* results in altered Purkinje cell morphology and is associated with the expression of a truncated *a2d-2* protein with abnormal function. *J Biol Chem* 277:7684–7693.
- Brown JP, Dissanayake VU, Briggs AR, Milic MR, Gee NS (1998) Isolation of the [ $^3\text{H}$ ]gabapentin-binding protein/ $\alpha_2\delta$   $\text{Ca}^{2+}$  channel subunit from porcine brain: development of a radioligand binding assay for  $\alpha_2\delta$  subunits using [ $^3\text{H}$ ]leucine. *Anal Biochem* 255:236–243.
- Canti C, Nieto-Rostro M, Foucault I, Heblch F, Wratten J, Richards MW, Hendrich J, Douglas L, Page KM, Davies A, Dolphin AC (2005) The metal-ion-dependent adhesion site in the Von Willebrand factor-A domain of  $\alpha_2\delta$  subunits is key to trafficking voltage-gated  $\text{Ca}^{2+}$  channels. *Proc Natl Acad Sci U S A* 102:11230–11235.
- Catterall WA (2000) Structure and regulation of voltage-gated  $\text{Ca}^{2+}$  channels. *Annu Rev Cell Dev Biol* 16:521–555.
- Cheng JK, Chiou LC (2006) Mechanisms of the antinociceptive action of gabapentin. *J Pharmacol Sci* 100:471–486.
- Coderre TJ, Kumar N, Lefebvre CD, Yu JS (2005) Evidence that gabapentin reduces neuropathic pain by inhibiting the spinal release of glutamate. *J Neurochem* 94:1131–1139.
- Costigan M, Befort K, Karchewski L, Griffin RS, D'Urso D, Allchorne A, Sitariski J, Mannion JW, Pratt RE, Woolf CJ (2002) Replicate high-density rat genome oligonucleotide microarrays reveal hundreds of regulated genes in the dorsal root ganglion after peripheral nerve injury. *BMC Neurosci* 3:16.
- Davies A, Douglas L, Hendrich J, Wratten J, Tran Van Minh A, Foucault I, Koch D, Pratt WS, Saibil HR, Dolphin AC (2006) The calcium channel  $\alpha_2\delta$ -2 subunit partitions with  $\text{Ca}_v2.1$  in lipid rafts in cerebellum: implications for localization and function. *J Neurosci* 26:8748–8757.
- Davies A, Hendrich J, Van Minh AT, Wratten J, Douglas L, Dolphin AC (2007) Functional biology of the  $\alpha(2)\delta$  subunits of voltage-gated calcium channels. *Trends Pharmacol Sci* 28:220–228.
- Dickenson AH, Matthews EA, Suzuki R (2002) Neurobiology of neuropathic pain: mode of action of anticonvulsants. *Eur J Pain* 6 [Suppl A]:51–60.
- Dolphin AC (2003)  $\beta$  subunits of voltage-gated calcium channels. *J Bioeng Biomemb* 35:599–620.
- Donato R, Page KM, Koch D, Nieto-Rostro M, Foucault I, Davies A, Wilkinson T, Rees M, Edwards FA, Dolphin AC (2006) The ducky2J mutation in *Cacna2d2* results in reduced spontaneous Purkinje cell activity and altered gene expression. *J Neurosci* 26:12576–12586.
- Field MJ, Oles RJ, Singh L (2001) Pregabalin may represent a novel class of anxiolytic agents with a broad spectrum of activity. *Br J Pharmacol* 132:1–4.
- Field MJ, Cox PJ, Stott E, Melrose H, Offord J, Su TZ, Bramwell S, Corradini L, England S, Winks J, Kinloch RA, Hendrich J, Dolphin AC, Webb T, Williams D (2006) Identification of the  $\alpha_2\delta$ -1 subunit of voltage-dependent calcium channels as a novel molecular target for pain mediating the analgesic actions of pregabalin. *Proc Natl Acad Sci U S A* 103:17537–17542.
- Fox A, Gentry C, Patel S, Kesingland A, Bevan S (2003) Comparative activity of the anti-convulsants oxcarbazepine, carbamazepine, lamotrigine and gabapentin in a model of neuropathic pain in the rat and guinea-pig. *Pain* 105:355–362.
- Glebov OO, Bright NA, Nichols BJ (2006) Flotillin-1 defines a clathrin-independent endocytic pathway in mammalian cells. *Nat Cell Biol* 8:46–54.
- Hao JX, Xu XJ, Urban L, Wiesenfeld-Hallin Z (2000) Repeated administration of systemic gabapentin alleviates allodynia-like behaviors in spinally injured rats. *Neurosci Lett* 280:211–214.
- Heblch F, Tran Van Minh A, Hendrich J, Watschinger K, Dolphin AC (2008) Time course and specificity of the pharmacological disruption of the trafficking of voltage-gated calcium channels by gabapentin. *Channels* 2:4–9.
- Hendrich J, Van Minh AT, Heblch F, Nieto-Rostro M, Watschinger K, Striessnig J, Wratten J, Davies A, Dolphin AC (2008) Pharmacological disruption of calcium channel trafficking by the  $\alpha_2\delta$  ligand gabapentin. *Proc Natl Acad Sci U S A* 105:3628–3633.
- Jones LP, Wei SK, Yue DT (1998) Mechanism of auxiliary subunit modulation of neuronal  $\alpha_{1E}$  calcium channels. *J Gen Physiol* 112:125–143.
- Kim SH, Chung JM (1992) An experimental model for peripheral neuropathy produced by segmental spinal nerve ligation in the rat. *Pain* 50:355–363.
- Klugbauer N, Marais E, Hofmann F (2003) Calcium channel  $\alpha_2\delta$  subunits: differential expression, function, and drug binding. *J Bioenerg Biomembr* 35:639–647.
- Li CY, Song YH, Higuera ES, Luo ZD (2004) Spinal dorsal horn calcium channel  $\alpha_2\delta$ -1 subunit upregulation contributes to peripheral nerve injury-induced tactile allodynia. *J Neurosci* 24:8494–8499.
- Li CY, Zhang XL, Matthews EA, Li KW, Kurwa A, Boroujerdi A, Gross J, Gold MS, Dickenson AH, Feng G, Luo ZD (2006) Calcium channel  $\alpha(2)\delta(1)$  subunit mediates spinal hyperexcitability in pain modulation. *Pain* 125:20–34.
- Lujan R, Nusser Z, Roberts JD, Shigemoto R, Somogyi P (1996) Perisynaptic location of metabotropic glutamate receptors mGluR1 and mGluR5 on dendrites and dendritic spines in the rat hippocampus. *Eur J Neurosci* 8:1488–1500.
- Luo ZD, Chaplan SR, Higuera ES, Sorkin LS, Stauderman KA, Williams ME, Yaksh TL (2001) Upregulation of dorsal root ganglion  $\alpha_2\delta$  calcium channel subunit and its correlation with allodynia in spinal nerve-injured rats. *J Neurosci* 21:1868–1875.
- Maneuf YP, McKnight AT (2001) Block by gabapentin of the facilitation of glutamate release from rat trigeminal nucleus following activation of protein kinase C or adenylyl cyclase. *Br J Pharmacol* 134:237–240.
- Melrose HL, Kinloch RA, Cox PJ, Field MJ, Collins D, Williams D (2007) [ $^3\text{H}$ ]Pregabalin binding is increased in ipsilateral dorsal horn following chronic constriction injury. *Neurosci Lett* 417:187–192.
- Miki K, Fukuoka T, Tokunaga A, Kondo E, Dai Y, Noguchi K (2000) Differential effect of brain-derived neurotrophic factor on high-threshold mechanosensitivity in a rat neuropathic pain model. *Neurosci Lett* 278:85–88.
- Moore KA, Baba H, Woolf CJ (2002) Gabapentin—actions on adult superficial dorsal horn neurons. *Neuropharmacology* 43:1077–1081.
- Newton RA, Bingham S, Case PC, Sanger GJ, Lawson SN (2001) Dorsal root ganglion neurons show increased expression of the calcium channel  $\alpha_2\delta$ -1 subunit following partial sciatic nerve injury. *Brain Res Mol Brain Res* 95:1–8.
- Page KM, Heblch F, Davies A, Butcher AJ, Leroy J, Bertaso F, Pratt WS, Dolphin AC (2004) Dominant-negative calcium channel suppression by truncated constructs involves a kinase implicated in the unfolded protein response. *J Neurosci* 24:5400–5409.
- Patel MK, Gonzalez MI, Bramwell S, Pinnock RD, Lee K (2000) Gabapentin inhibits excitatory synaptic transmission in the hyperalgesic spinal cord. *Br J Pharmacol* 130:1731–1734.
- Paxinos G, Watson C (2005) The rat brain in stereotaxic coordinates. Amsterdam: Elsevier.
- Pitcher GM, Henry JL (2004) Nociceptive response to innocuous mechanical stimulation is mediated via myelinated afferents and NK-1 receptor activation in a rat model of neuropathic pain. *Exp Neurol* 186:173–197.

- Qin N, Olcese R, Stefani E, Birnbaumer L (1998) Modulation of human neuronal  $\alpha_{1E}$ -type calcium channel by  $\alpha_2\delta$ -subunit. *Am J Physiol* 274:C1324–C1331.
- Shehab SA, Al-Marashda K, Al-Zahmi A, Abdul-Kareem A, Al-Sultan MA (2008) Unmyelinated primary afferents from adjacent spinal nerves intermingle in the spinal dorsal horn: a possible mechanism contributing to neuropathic pain. *Brain Res* 1208:111–119.
- Snutch TP (2005) Targeting chronic and neuropathic pain: the N-type calcium channel comes of age. *NeuroRx* 2:662–670.
- Sun H, Ren K, Zhong CM, Ossipov MH, Malan TP, Lai J, Porreca F (2001) Nerve injury-induced tactile allodynia is mediated via ascending spinal dorsal column projections. *Pain* 90:105–111.
- Suzuki R, Rygh LJ, Dickenson AH (2004) Bad news from the brain: descending 5-HT pathways that control spinal pain processing. *Trends Pharmacol Sci* 25:613–617.
- Suzuki R, Rahman W, Rygh LJ, Webber M, Hunt SP, Dickenson AH (2005) Spinal-supraspinal serotonergic circuits regulating neuropathic pain and its treatment with gabapentin. *Pain* 117:292–303.
- Svensson CI, Yaksh TL (2002) The spinal phospholipase-cyclooxygenase-prostanoid cascade in nociceptive processing. *Annu Rev Pharmacol Toxicol* 42:553–583.
- Wang H, Sun H, Della PK, Benz RJ, Xu J, Gerhold DL, Holder DJ, Koblan KS (2002) Chronic neuropathic pain is accompanied by global changes in gene expression and shares pathobiology with neurodegenerative diseases. *Neuroscience* 114:529–546.
- Woolf CJ, Fitzgerald M (1986) Somatotopic organization of cutaneous afferent terminals and dorsal horn neuronal receptive fields in the superficial and deep laminae of the rat lumbar spinal cord. *J Comp Neurol* 251:517–531.
- Wyatt CN, Page KM, Berrow NS, Brice NL, Dolphin AC (1998) The effect of overexpression of auxiliary calcium channel subunits on native  $Ca^{2+}$  channel currents in undifferentiated NG108–15 cells. *J Physiol* 510:347–360.
- Xiao W, Boroujerdi A, Bennett GJ, Luo ZD (2007) Chemotherapy-evoked painful peripheral neuropathy: analgesic effects of gabapentin and effects on expression of the alpha-2-delta type-1 calcium channel subunit. *Neuroscience* 144:714–720.
- Yoon MH, Yaksh TL (1999) The effect of intrathecal gabapentin on pain behavior and hemodynamics on the formalin test in the rat. *Anesth Analg* 89:434–439.
- Yusaf SP, Goodman J, Gonzalez IM, Bramwell S, Pinnock RD, Dixon AK, Lee K (2001) Streptozocin-induced neuropathy is associated with altered expression of voltage-gated calcium channel subunit mRNAs in rat dorsal root ganglion neurones. *Biochem Biophys Res Commun* 289:402–406.
- Zhang Y, Helm JS, Senatore A, Spafford JD, Kaczmarek LK, Jonas EA (2008) PKC-induced intracellular trafficking of  $Ca_v2$  precedes its rapid recruitment to the plasma membrane. *J Neurosci* 28:2601–2612.
- Zimmermann M (1983) Ethical guidelines for investigations of experimental pain in conscious animals. *Pain* 16:109–110.